République Algérienne Démocratique et Populaire

Ministère de l'enseignement supérieur et la recherche scientifique

École Nationale Polytechnique

Department of Electronics

Laboratoire des Dispositifs de Communication et de Conversion Photovoltaïque

Doctoral Thesis

In: Electronic

PV array power output maximization under partial shading using new configurations and arrangements

Presented by :

BELHAOUAS Nasreddine

Magister in Renewable Energies at ENP

Under supervision of M. AIT CHEIKH Mohamed Salah, Professor

Presented and defended publicly the 04 october2017

Composition of the Jury:

President:	**M.HADDADI Mourad,**	Professor	ENP, Algeria
Supervisor:	**M.AIT CHEIKH Mohamed Salah,**	Professor	ENP, Algeria
Examiner:	**M.LARBES Chérif,**	Professor	ENP, Algeria
Examiner:	**M.HADJ ARAB Amar,**	Rech.Dir	CDER, Algeria
Examiner:	**Mme.BARAZANE Linda,**	Professor	USTHB, Algeria
Examiner:	**Mme.BOUKHELIFA Akila,**	MCA	USTHB, Algeria
Invited :	**Mme.AMROUCHE Badia,**	MRA	CDER, Algeria

ENP-2017

———————————————————————————-

10 Avenue des frères Oudek, Hassen Badi BP 182,16200 El Harrach, Alger, Algérie

www.enp.edu.dz

République Algérienne Démocratique et Populaire

Ministère de l'enseignement supérieur et la recherche scientifique

École Nationale Polytechnique

Department of Electronics

Laboratoire des Dispositifs de Communication et de Conversion Photovoltaïque

Doctoral Thesis

In: Electronic

PV array power output maximization under partial shading using new configurations and arrangements

Presented by :

BELHAOUAS Nasreddine

Magister in Renewable Energies at ENP

Under supervision of M. AIT CHEIKH Mohamed Salah, Professor

Presented and defended publicly the 04 october2017

Composition of the Jury:

President:	**M.HADDADI Mourad,**	Professor	ENP, Algeria
Supervisor:	**M.AIT CHEIKH Mohamed Salah,**	Professor	ENP, Algeria
Examiner:	**M.LARBES Chérif,**	Professor	ENP, Algeria
Examiner:	**M.HADJ ARAB Amar,**	Rech.Dir	CDER, Algeria
Examiner:	**Mme.BARAZANE Linda,**	Professor	USTHB, Algeria
Examiner:	**Mme.BOUKHELIFA Akila,**	MCA	USTHB, Algeria
Invited :	**Mme.AMROUCHE Badia,**	MRA	CDER, Algeria

ENP-2017

———————————————————————————-

10 Avenue des frères Oudek, Hassen Badi BP 182,16200 El Harrach, Alger, Algérie

www.enp.edu.dz

DEDICATION AND ACKNOWLEDGEMENTS

This thesis would not have been a possibility if it did not have the guidance and support of some peoples; the people I am going to name have one way or the other added life to this work.

First, I owe my deepest gratitude to my principal advisor, Professor Mohamed Salah AIT CHEIKH at ENP in Algeria, who has been advising and supporting me from the very beginning of this thesis work until its very end.

The Professors Ned DJILALI and Pan AGATHOKLIS from Victoria University in Canada, Badia AMROUCHE at CDER in Algeria, words that helped me understand the subject to great lengths. I truly appreciate all theirs contributions of time, brilliant ideas, theirs expert supervision, and extensive knowledge of this subject.

This acknowledgment would not be completed without the mention of my thesis committee: Professors Mourad HADDADI at ENP, Cherif LARBES at ENP, Amar HADJ ARAB at CDER ,Linda BARAZANE at USTHB in Algeria and Akila BOUKHELIFA at USTHB for their time and insightful comments. I am indebted and thankful to all of you Professors in the jury,who graciously guided me to the end of this thesis work.

My family has been a plethora of support for me and I would like to extend my gratitude and love to them for their understanding and endless love, through the duration of my studies.

ملخص

الظل الجزئي يمكن أن يقلل بشكل كبير إنتاج الطاقة الكهروضوئية وكذلك عملية تصبح أكثر تعقيد من خلال التسبب في تشكيل ذروة متعددة في منحنى استطاعة تيار. هذه المشاكل لا تعتمد فقط على منطقة الظل ولكن أكثر من ذلك بكثير إلى شكل الظل . في هذا العمل تم اقتراح ثلاثة الترتيبات جديدة مطبقة على مصفوفة كهر وضوئية للتخفيف تأثيرأضرار الظل الجزئي . وتستند هذه الترتيبات على تحقيق أقصى قدر من المسافة بين الوحدات الكهروضوئية المجاورة، بينما يتم ترتيب وحدات لتكون في مختلف الصفوف والأعمدة دون تغيير التوصيلات الكهربائية. وهذا يسمح إعادة توزيع أنماط الظل على مصفوفة كهر وضوئية بأكملها، ويؤدي ذلك إلى التقليل من الثنائيات حماية من تبديد الطاقة بالإضافة إلى زيادة إنتاج الطاقة والقضاء على قمم متعددة.يتم عرض المحاكاة لتقييم الترتيبات المقترحة ومقارنة الأداء مع مختلف تكوينات والترتيبات وفقا أنماط الظل وسيناريوهات مختلفة. الترتيبات الجديدة لها مستوى علي من الأداء من حيث إنتاج الطاقة، وفق ذلك تمكننا من القضاء على المشكلة من قمم متعددة.

كلمات مفاتيح: طاقة شمسية,الطاقة الكهروضوئية ,الظل الجزئي ,الثنائيات,الترتيبات, نقطة الاستطاعة القصوى

Résumé

L'ombrage partiel peut réduire considérablement la puissance d'un champ photovoltaïque ainsi que provoquer l'apparition de pics dans la courbe caractéristique puissance tension (P-V). Ces problèmes ne dépendent pas seulement de la quantité d'ombrage, mais beaucoup plus de la forme d'ombrage. Dans ce travail, trois nouveaux arrangements physiques sont appliqués sur un champ photovoltaïque afin d'atténuer l'effet d'ombrage partiel. Les arrangements sont basés sur la maximisation de la distance entre les modules PV adjacents d'un champ, tout en disposant les modules pour être dans des lignées et des colonnes différentes sans changer les connexions électriques initiales. Cela permet la redistribution de la forme d'ombrage sur l'ensemble d'un champ PV d'une façon uniforme, cela entraîne une minimisation de la perte de puissance du aux diodes de protection, en plus de maximiser la puissance de sortie du champ PV et d'éliminer l'apparition des multi pics sur la courbe (P-V). Des simulations sont présentées afin d'évaluer les arrangements physiques proposés. Cette évaluation est faite à travers une comparaison des performances pour diverses configurations et arrangements sous différents modèles et scénarios d'ombrage.

Mots clés : Energie solaire, photovltaique (PV), Effet de L'ombrage partiel, diodes by-pass et anti retour, Champ PV configuration, Poursuite de point de puissance maximale (MPPT).

Abstract

Partial shading can dramatically decrease PV array power output as wellas complicate operation by causing multiple peak exhibitions in the power voltage (P-V) characteristic curve. These problems depend not only on the shading area but also and much more significantly on the shading pattern. In this work three new physical PV array arrangements to mitigate partial shading effects, are proposed. These arrangements are based on maximizing the distance between adjacent PV modules within a PV array, while rearranging modules to be in different rows and columns without changing the electrical connections. This allows redistribution of the shading patterns over the entire array. This result in a power dissipation minimization of the protection diodes in addition to maximizing the power output and eliminating multi peaks. Simulations are presented to assess the proposed physical PV array arrangements. This assessment is done through performance comparisons for various PV array configurations and arrangements under different shading patterns and scenarios. The new physical PV array arrangements yields the highest performance in terms of power output and eliminates the problem of local multi peaks in the P-V array characteristic curve.

Keywords: **Solar energy, Photovoltaic (PV), partial shading effects, Bypass and blocking diodes, PV array configuration, Maximum power point tracking (MPPT).**

Table of Contents

Page

List of Figures

Figure **Page**

List of Tables

Table **Page**

List of Acronyms and Abbreviations

PV Photovoltaic.

MPP Maximum power point [W/m2].

LMPP Local maximum power point [W/m2].

GMPP Global Maximum power point [W/m2].

MPPT Maximum power point tracking.

V_{mp} Voltage at the maximum point [V].

I_{mp} Current at the maximum point [A].

STC Standard test conditions.

Iph (STC) Photo current at STC [A].

T(STC) PV Cell temperature at STC[K].

T PV Cell temperature at STC[K].

G(STC) Irradiance at STC [W/m2].

G Solar irradiance in [W/m2].

K_i Temperature short circuit coefficient.

I_0 The reverse saturation current [A].

q Electron charge(1.60210-19C).

k Boltzmann constant (1.3810-23J/K).

A_i Diode ideality constants.

R_s Series resistance [Ω].

R_p Parallel resistance [Ω].

N_{cell} Number of series cells.

I_{0i} Reverse saturation current [A].

a_i Diode ideality factor.

EAR Electrical Array Reconfiguration.

SW Short Wide shadow type.

SN Short Narrow shadow type.

LW Long Wide shadow type.

LN Long Narrow shadow type.

SP Serie-parrallel configuration.

BL Bridge-link configuration.

HC Honey comb configuration.

TCT Total cross tied configuration.

M-TCT Modified TCT arrangement.

S-M-TCT Shift modified TCT arrangement.

// **S-M-TCT** Parallel shift modified TCT arrangement.

S-M-TCT+BLK Shift modified TCT arrangement with the blocking diode.

General introduction

Solar energy is one of the fastest growing renewable energy resources [2, 3]. Solar power generation is economically and environmentally attractive for meeting growth in electricity demand and reducing reliance on fossil fuels; however, several challenges need to be addressed to allow its effective deployment [4].
The power output of photovoltaic (PV) cells arrays, the focus of this work, is optimal only if an array is fully irradiated. when it is not, the efficiency of the PV array can decrease dramatically. A decrease, in solar irradiance during operation, is mostly caused by partial shading [5]. The extent and impact of shading depends on the end use application, e.g. solar PV power plants, building-integrated photovoltaic, rural electrification or electric vehicle. Alleviating the effect of partial shading is an important practical challenge due to its significant impact on the efficiency of PV array systems [6, 7]. In addition to reducing the PV array power output, partial shading also causes the power-voltage (P-V) curve to exhibit multiple peaks. As a result, this can cause conventional Maximum Power Point Tracking (MPPT) techniques to be trapped at a Local Maximum Power Point (LMPP), which leads to significant power losses. Sophisticated MPPT algorithms have been devised to address this problem and reach the Global Maximum Power Point (GMPP) [8, 9]. These algorithms are unfortunately complex and costly, and in some cases require embedded sensors [10, 11].
PV output power losses depend more on the shading pattern rather than shaded area [12]. Researchers tried to overcome the power losses caused by the partial shading effect using electrical configurations based on interleaving the PV modules [13]. Some works as [14] has shown that partial shading losses can be reduced by modifying the

electrical configuration of the P-V array, opening a whole area of research. Another configuration modification approach is the Electrical Array Reconfiguration (EAR), consists of dynamically changing the electrical connections of PV modules. This strategy requires a fully reconfigurable array and necessitates sensors and switches necessary which increases the system complexity and cost [1, 15].

In this work a new electrical connection pattern is proposed by connecting modules that are far apart but not on the same row and/or column [16, 17]. The shaded PV modules are thereby distributed over the entire PV array. The proposed PV array arrangement leads to P-V characteristic curves with only one peak which corresponds to the GMPP. The proposed arrangement makes it easy to find the GMPP and thus maximize power output. This proposed arrangement helps reshape the P-V characteristic to ensure one peak even under severe partial shading conditions. The protection diode configuration combined with the proposed array arrangement is investigated and analyzed under a variety of shading patterns. We show that the proposed approach leads to i) PV curves with one peak leading to easy identification of GMPP; ii) Maximize PV array power output. iii) Reduces power dissipation by the protection diodes.

Our work is arranged as follows: In chapter I, an overview of the PV system where a description of the important parts are given. Chapter II gives an analysis of the partial shading effect and its impact at different stage of the PV system. Chapter III reports and analyzes different PV array configurations in order to increase the PV array power output and the power dissipation under shading condition. it gives detail description of the different proposed PV array configurations and their efficiency to distribute the shading pattern. The proposed PV array arrangements with different PV array configurations and recent PV array arrangement under different shading pattern and scenarios in chapter IV are discussed and compared. The conclusion of this work and the contribution of the presented PV array arrangement to minimize partial shading effect and increase the efficiency of conventional MPPT algorithm to track MPP are given at the end of this thesis work.

CHAPTER 1

PHOTOVOLTAIC SYSTEM OVERVIEW

1.1 Introduction

This chapter is dedicated to the main concepts of photovoltaic system. it explains the current visions of the photovoltaic system in literature. Understanding photovoltaic system and being able to model each part of it, presents an essential step to start the photovoltaic system analysis. Many challenges are facing users of photovoltaic systems under different aspect mainly including cells, modules and arrays modeling, characteristic curves setting out, MPPT controller . . . etc.

The current literature is reviewed for several models, theory and a method comparing its different contributions. Based on this comparison, potentially interesting PV models and techniques for each part of PV system are chosen and selected which leads to a useful tool for the full comprehension of the concepts described in the following chapters of this thesis. This chapter is devoted to the description of the PV generator system operation, in different weather conditions.

1.2 PV cell Modeling

The photovoltaic cell model is a nonlinear model and its output depends essentially on sunlight and temperature.

Different equivalent circuits have been developed in the literature in order to assess the behavior of the PV cell [18]. In our study, we consider the two-diode model which provides an even better description of the solar cell [18, 19]. The two-diode model is depicted in Fig.1.1. Using Kirchhoff's first law, the output current of the cell is drawn from Fig.1.1:

A PV module consists of many jointly connected PV cells. The equivalent module circuit equation for an (Ncell) PV cells in series, leads to the eqt.1.1 [20, 21].

$$I = I_{Ph} - I_{d1} - I_{d2} - \frac{V + IR_S N_{cell}}{R_p N_{cell}} \tag{1.1}$$

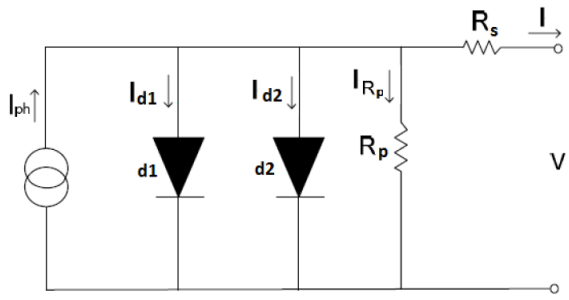

Figure 1.1: Equivalent two-diode circuit model of a PV cell.

$$I_{Ph} = (I_{Ph(STC)} + K_i(T - T_{(STC)}))\frac{G}{G_{(STC)}} \tag{1.2}$$

$$I_{d,i=1,2} = I_{0i} \exp\left(\frac{V + IR_S N_{cell}}{A_i\left(\frac{KT}{q}\right)N_{cell}}\right) \tag{1.3}$$

with the variables and parameters represented, in the standard test conditions (STC) by:

STC : standard test conditions.

$I_{Ph(STC)}$: photo current at STC [A].

$T_{(STC)}$: PV Cell temperature at STC[K].

T: PV Cell temperature [K].

$G_{(STC)}$: irradiance at STC [W/m^2].

G: solar irradiance in [W/m^2].

K_i: temperature short circuit coefficient.

I_0: reverse saturation current[A].

q: electron charge($1.60210^{-19}C$).

k: Boltzmann constant ($1.3810^{-23}J/K$).

A_i: diode ideality constants.

R_s: series resistance [Ω].

R_p: parallel resistance [Ω].

N_{cell}: number of series cells.

I_{0i}: reverse saturation current.

A_i: diode ideality factor.

All PV module datasheets bring basic information with reference to the standard test conditions (STCs). Some of the parameters, required for adjusting PV system models, such as Rs and Rp, are not specified. So, to use a more accurate model, these parameters are calculated simultaneously [22]. The model is obtained with the parameters of the $I-V$ equation given by manufacturer datasheet such as open-circuit voltage V_{oc}; short-circuit current Isc, maximum output power Pmax, voltage and current at the maximum power point (V_{mpp}, I_{mpp}) [23]. The relation between Ipv and Isc replaces the assumption that Ipv is equal to Isc. The two diodes model given in this work present a good PV characteristic and $I-V$ curve. However, this is done through Newton-Raphson algorithm in order to compute , from eqt.1.1 , the module output current [24].

Newton-Raphson algorithm has the advantage of a very quick convergence especially when the initial values are chosen near to the root, as given in eqt.1.4 . So, after few iteration steps, a occurrence solution, of Rp in function of Rs as in eqt.1.5 , is computed until the maximum experimental power value coincides with the (V_{mpp}, I_{mpp}) maximum power point,$P_{max,m} = P_{max,e}$, found in the corresponding module datasheet [25], the variable p can be chosen to be P>2,2 in order to match between this PV model and practical I-V curve [21].

$$R_{p0} = \left(\frac{V_{mp}}{I_{sc} - I_{mp}}\right) - \left(\frac{V_{oc} - V_{mp}}{I_{mp}}\right) \tag{1.4}$$

$$R_p = \frac{V_{mp} + I_{mp}R_s}{I_{pv} - I_0\left[\exp\left(\frac{V_{mp}+I_{mp}R_S}{\left(\frac{KT}{q}\right)}\right) - \exp\left(\frac{V_{mp}+I_{mp}R_S}{(p-1)\left(\frac{KT}{q}\right)}\right) - 2\right] - \frac{P_{max,e}}{V_{mp}}} \tag{1.5}$$

1.3 Modeling the photovoltaic array

Usually PV cells are connected in series to form a PV module and the PV modules are then connected in series to form a string. Finally, the strings are connected in parallel

to form a PV array; in other words, this is can be done by connecting PV modules in series and parallel. Hence, the PV array modeling can be compute easily base on the PV cell model equations [26].

The PV array size is specified according to the required voltage, current and power produced at the terminals of PV array [27].

Generally, PV arrays have protection diodes, called bypass and blocking diode, connected in parallel with each individual module and series with PV string respectively, as shown in Fig .1.2.

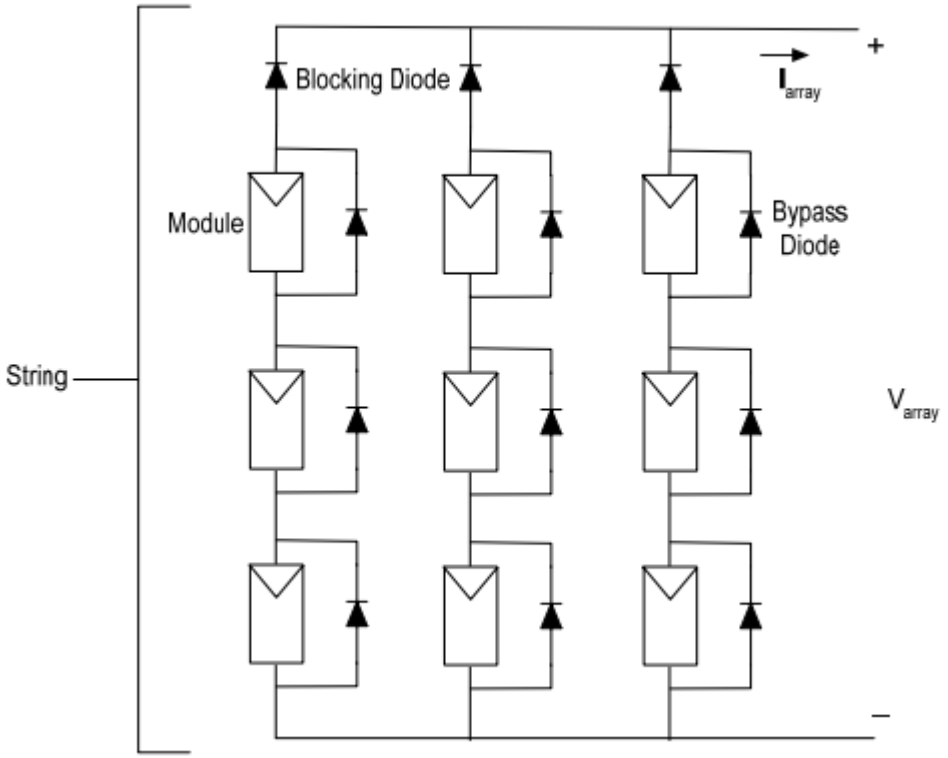

Figure 1.2: PV array Structure.

1.4 PV characteristic curves

The photovoltaic effect, described by the above equations, defines a non-linear dependency between current and voltage. This dependency is expressed by the current versus voltage and the power versus voltage curves [28, 28].
The characteristics of a photovoltaic cell/module strongly depend on irradiance and temperature as seen in the eqt.1.2. This becomes very apparent when the PV characteristic equations for selected values of temperature and irradiance are evaluated and plotted Fig.1.3 and 1.4 [29].

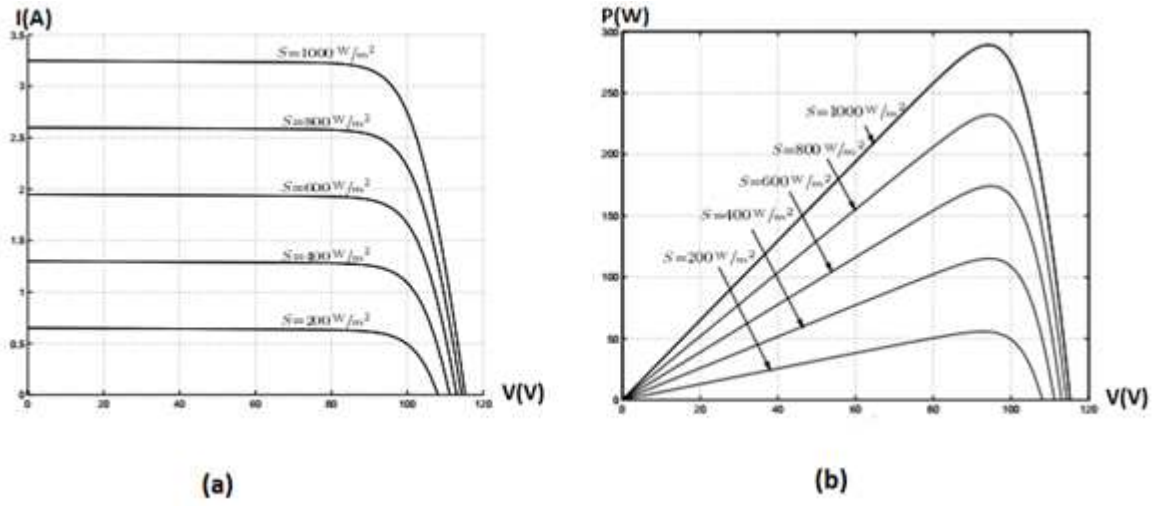

Figure 1.3: PV characteristic under various irradiances value S: (a) I-V curve. (b) P-V curve.

Fig.1.3 shows that the PV output current is greatly influenced by the change in irradiance, whereas the output voltage stays approximately constant. In contrast, for a changing temperature one can see that the voltage varies widely while the current remains almost unchanged as seen in Fig.1.4.

In addition, the PV power output not only depends on temperature and irradiance, but also very strongly on its operating voltage. The point of maximum power indicated as MPP (Maximum Power Point) in Fig.1.5 is the desired operating point for a

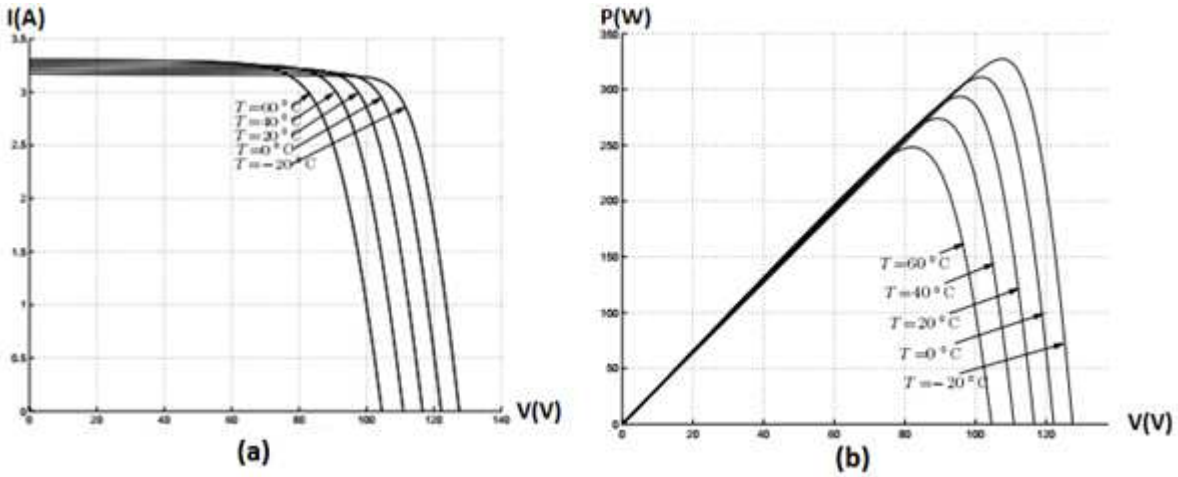

Figure 1.4: PV characteristic under various temperatures: PV value T: (a) I-V curve. (b) P-V curve.

photovoltaic array to obtain maximum efficiency [9]. The corresponding values for voltage and current are called V_{mp} and I_{mp}, respectively.

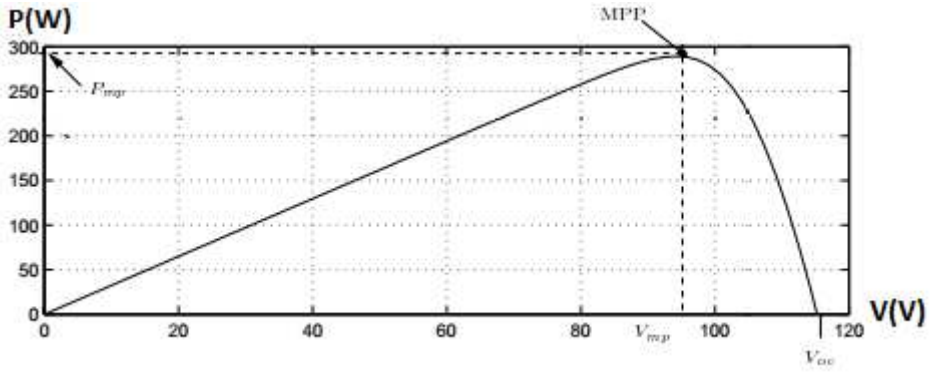

Figure 1.5: Maximum power point and the corresponding V_{mp} and I_{mp} for PV characteristic.

1.5 Maximal power point tracking (MPPT)

The MPP tracking is necessary to maximize the PV power output whatever the electrical values (V_{mpp} and I_{mpp}) and weather conditions. The objective of the

electrical tracking of MPP is achieved through power conditioning converters as an interface between the load and PV source as shown in Fig.1.6. The switching converters are suitably controlled to change the load impedance to the required one to achieve for the MPPT under the given environmental condition.

There are several algorithms for the control of power converters to track MPP. Some of the widely used schemes are the Perturb and Observe ($P\&O$) and incremental-conductance method (INC) [9, 30]. But these are slow tracking techniques and are not suitable for rapidly changing environmental conditions or particularly under partial shading effect [8]. A lot of power remains unutilized during tracking period due to slow speed. This, results in the requirement of fast and accurate method for tracking MPP [31]. Some advantages and disadvantages of each MPPT technique will be given in the coming section .

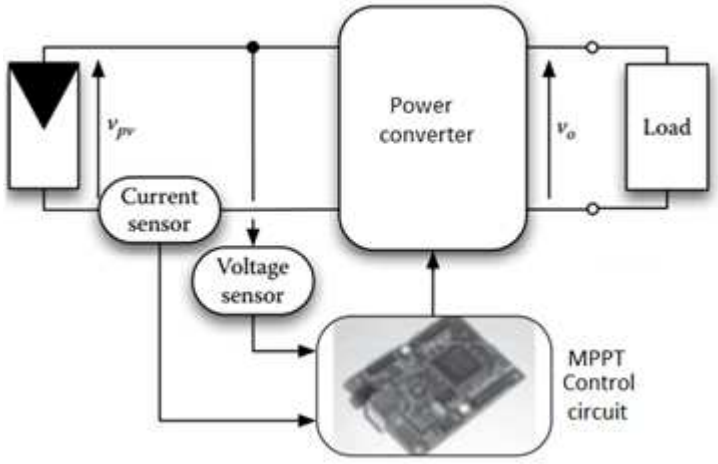

Figure 1.6: Structure of MPPT control for PV system.

1.6 MPPT controller and algorithm

Different MPPT controllers algorithms presented in the literature need in most cases the PV current and voltage values. Direct sensing of the temperature and irradiance is used for sophisticated MPPT controllers, as their measurement requires expensive

devices that have to be placed throughout the PV generator, thus making the measurement quite expensive [9].

Maximum power point controller allows operating the photovoltaic array at MPP. To do so, the MPPT adjust the pulse width of a power converter such as the DC/DC or DC/AC converter, as shown in Fig.1.6. The MPPT controller continuously adjusts the duty cycle to follow the MPP, based on the instantaneous values of the current and voltage sensed at the PV generator terminals for whatever irradiance and temperature operating conditions.

The practical implementation of MPPT controllers is mostly realized in digital form. The computations, required by MPPT algorithms allow the designer to use cheap microcontrollers, for basic P&O and INC approaches. It uses much more expensive devices, like digital signal processing (DSP) and/or Field-programmable gate array (FPGA) systems [32], when the MPPT approach is based on much more involved and difficult computations, as those required by neural networks, fuzzy logic and advanced techniques [33–35]. A comparison between MPPT techniques under different difficulties is given in the literature [30] .

1.6.1 Perturb and Observe algorithm

The perturb and observe (P&O) algorithm is the most popular algorithm; it is characterized by the injection of a small perturbation into the system, whose effects are used to drive the operating point (voltage, current) toward the MPP [36] .

The P&O algorithm is based on changing the Voltage at the PV terminals by perturbing the PV operating points periodically, and after each perturbation, the algorithm compares the values of the power produced by the PV source before and after the perturbation. For each perturbation made the PV power increases or decreases. Hence, if the PV power output has been increased that means that the operating point has been moved toward the MPP; consequently, the next perturbation will have the same sign as the previous one. If after a voltage perturbation the PV power output decreases, this means that the operating point has been moved away

from the MPP. Therefore, the sign of the next perturbation is reversed. Finally, if the oscillations of the operating point and sign of the perturbation is altering (+/-) it means that the MPP (V_{mpp}, I_{mpp}) is reached [37].

1.6.2 Incremental conductance algorithm

In the incremental conductance algorithm, the MPP is tracked by matching the PV array impedance with the effective impedance of the power converter reflected across the PV array terminals by increasing or decreasing voltage value perturbation [38, 39]. Mathematically, the algorithm can be explained as below:

$$\frac{\Delta I_{pv}}{\Delta V_{pv}} > -\frac{I_{pv}}{V_{pv}} \Rightarrow \text{ Increase voltage value perturbation.} \tag{1.6}$$

$$\frac{\Delta I_{pv}}{\Delta V_{pv}} < -\frac{I_{pv}}{V_{pv}} \Rightarrow \text{ Decrease voltage value perturbation .} \tag{1.7}$$

As a consequence, the method requires the application of a repeated perturbation of the voltage value, until the following condition occurs:

$$\frac{\Delta I_{pv}}{\Delta V_{pv}} = -\frac{I_{pv}}{V_{pv}}. \tag{1.8}$$

1.7 Conclusion

This chapter has proposed an overall study of the photovoltaic system. Its objective was to propose a short understanding of the photovoltaic system in literature. In additions, only the important techniques and problems in PV system have been pointed in order to address the challenges in the coming chapters of this work.

CHAPTER 2

ANALYSIS OF PARTIAL SHADING EFFECT

2.1 Introduction

The main objective of this chapter is to establish a clear relationship between partial shading effect, shadow pattern, PV array configuration and MPP of the PV system, in order to maximize PV system output.
Shading analysis is one of the most essential steps in PV system design or analysis. In photovoltaic, it is important to analyze the partial shading caused by surrounding obstacles or other such as weather conditions environments [40]. To minimize the influence of the partial shading effect in PV system different system optimization techniques have to be operate, since the partial shading effect on PV systems reduces dramatically their power output.

2.2 The partial shading effect

The partial shading effect is related to the power losses of a solar cell, module, or array operating under different weather conditions. These include soiling, poorly soldered cells, non-uniform irradiation, temperature variations, and cell cracking [41].
The partial shading effect regroups all conditions that lead to a change in the photocurrent of the PV module/array. These conditions reduce current production of the cell or module [42]. Thus, the modules, operating normally impose their higher current over any shaded PV module connected in series, forcing these into reverse bias and dissipating power. In addition, when the shaded PV module's temperature exceeds a critical value, allowed of PV cells in the PV module, cracking may occur. This phenomenon is called Hot Spot [43].

2.3 The Hot-spot heating formation

PV modules under partial shading effect within an unprotected PV array, can result in dissipating power as seen in the Fig.2.1. In the worst case, the whole output of the unshaded PV modules can be dissipated in the unprotected shaded PV modules,

especially when the PV array or string of PV modules is short-circuited due to the highest current [44].

Dissipation of power in shaded PV modules leads to breakdown in localized regions of the p-n junction cell . Enormous power dissipation can occur in a small area, leading to local overheating, also known as Hot Spots, which leads to destructive effects, such as cracking or melting in the shaded part. Similar effects occur to groups of cells, modules, or string within the PV array [43].

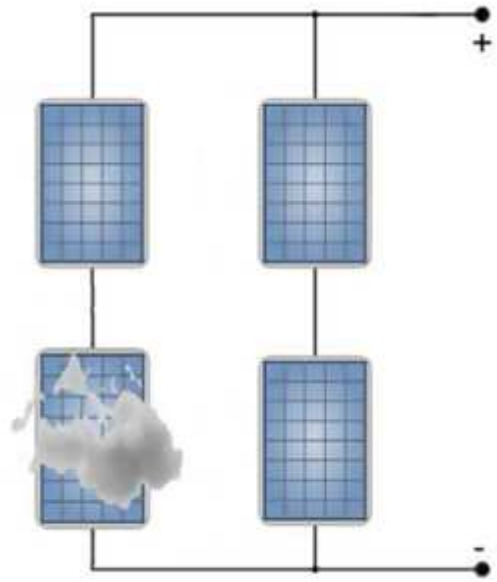

Figure 2.1: Unprotected 2x2 PV array with one shaded PV module.

2.4 The impact of the protection diodes to prevent the hot spot heating

One solution to the problem of hot spots and minimizing the partial shading effect in the PV system is to add protection diodes such as blocking and bypass diodes to the PV system. As shown in the Fig.2.2.

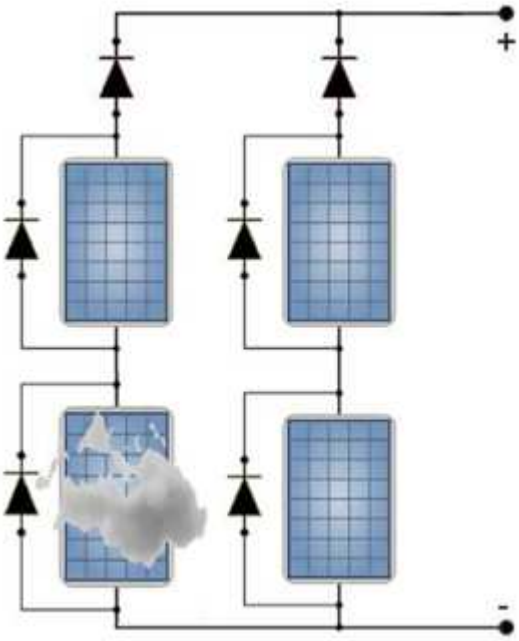

Figure 2.2: 2x2 PV array protected by bypass and blocking diode with a shaded PV module in PV string.

2.4.1 The bypass diodes impact

The bypass diode is reverse biased. When a PV module is shaded, it ceases to generate and acts as a high resistance and tends to be reverse-biased to the other PV modules, causing the bypass diode across the shaded PV module to conduct, thereby bypassing the shaded PV module [45].

The Fig.2.2 shows a bypass diodes connected to each PV module or group of PV cells, in a 2x2 PV array with a shaded PV module. The effect of these diodes is very considerable, since it allows to increase the PV array power output and protect the faulty PV module [6].

In practice, since one bypass diode per cell is generally too expensive, bypass diodes are usually placed across groups of cells. The maximum power dissipation in the shaded cell is then approximately equal to the generating capability of all cells in the same string or group. Not all commercial PV modules include bypass diodes. If they do not, care must be taken to ensure the modules are not short-circuited for long periods

and that parts of the module are not shaded by surrounding structures or adjacent PV modules [46]. As an example, the maximum silicon solar cells group size per bypass diode without causing damage is about 10 to 18 cells per bypass diode. Hence for a normal 36 cells divide in two equal parts in PV module, one or two bypass diodes are needed to ensure the module will not be vulnerable to hot spot damage.
The MSX-60 with 36 cells has been chosen as an example for this work. Note the developed GUI give the possibility to choose the number of bypass diode per cells as will be described in the coming sections.

2.4.2 The blocking diodes impact

The blocking diode is the one which is connected to a PV string in series as shown in Fig. 2.2. Blocking diodes are used to protect PV string from reverse current and ensure that the current flows out of the PV string. This prevents the current of an unshaded PV string to flow in the shaded PV string or when a battery is discharging through the PV modules during the night.
Furthermore, even during a uniform irradiance (without shading) small voltage drop is noticed due to forward biased of the blocking diode when it's conducting [44].

2.4.3 Impact of bypass and blocking diodes under partial shading

To recap, all PV modules within a PV array have the same characteristics. However the PV array power output is limited by the shaded modules that dissipate significant part of the generated power. The energy dissipated leads to overheating and hence damage and degradation of the shaded PV modules [47]. One solution is to add bypass diodes in reverse across each PV module.
The bypass diode is reverse biased when the PV module is generating power under uniform irradiance. However, under partial shading conditions the PV module tends to be reverse biased by other PV modules causing bypass conduction [46]. Thus, the

bypass diodes will short-circuit the shaded PV module allowing the current to flow through them, thereby reducing the power loss through the shaded PV modules.
In practice, typical power dissipation of the PV array with bypass protection is illustrated in Fig. 2.3, showing a simulation of a PV string corresponding to the shaded and unshaded PV modules in Fig. 2.4(a).

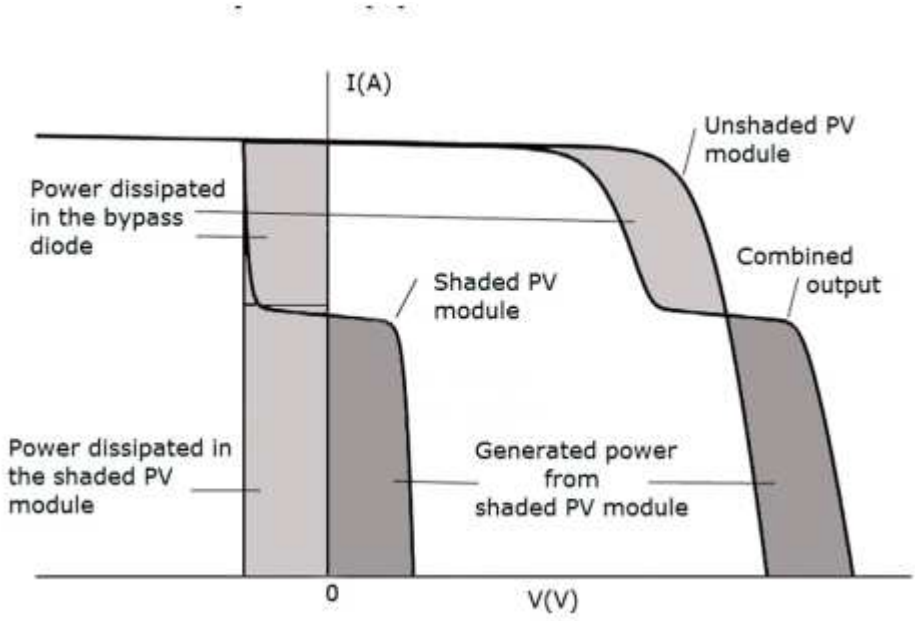

Figure 2.3: Impact of bypass diode on the (I-V) PV characteristic of two PV modules connected in series.

The combined I-V curves, Fig. 2.3, obtained by summing individual PV modules I-V curves, include the voltage when conducting current. Fig. 2.3 illustrates the power dissipated in the bypass diode and the shaded PV module. The dissipation power drawn in light gray in Fig. 2.3 depends on the severity of the shading, diode current conduction, and number of shaded cells per bypass diode. Since power dissipation increases with increasing current, through a bypass diode, it is effective to minimize this current by minimizing the number of PV module in a string under TCT configuration. The reduced power dissipation in the shaded PV modules is also beneficial in reducing the number of cells per bypass diode or the number of PV modules per string.

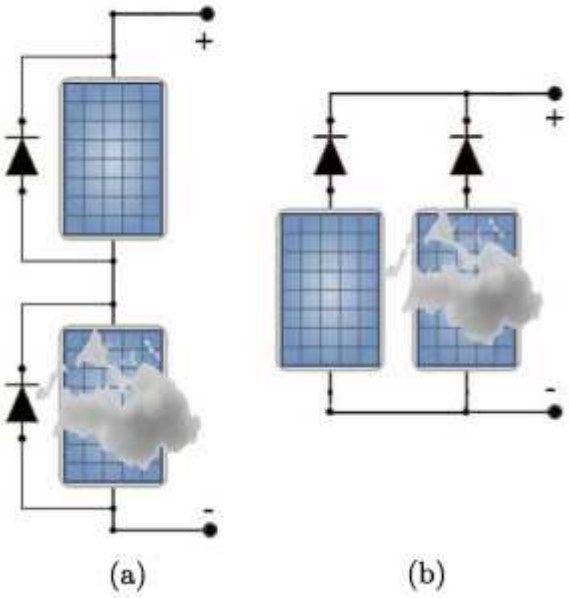

Figure 2.4: Two PV modules (one of which is shaded) connected in (a) series with bypass diodes protection, (b) parallel with blocking diodes protection.

Hot spot problems may arise in other ways, e.g. when strings or PV modules are wired in parallel and one of them is shaded. Instead of generating power, such a module would dissipate the power generated by other unshaded modules [48]. This problem can be solved by adding blocking diodes on the top of each string in an SP configuration or on each PV module in TCT configuration Fig.2.5, thus preventing the reverse current flow through shaded PV modules. Fig.2.6 shows the I-V characteristic curve of two PV modules connected in parallel one of which is partially shaded as in Fig. 2.4 (b). The importance of inserting a blocking diode in each PV module, within a PV array connected in TCT configuration (Fig.2.5(b)) is illustrated in Fig.2.6. For modules in parallel, as shown in Fig. 2.4, an additional problem, thermal runaway, can occur when bypass diodes are used. One string of bypass diodes becomes hotter than the rest, therefore taking up a larger share of the current, hence becoming even hotter and so on. Diodes should therefore be rated to handle the parallel current of the module combination. However, in this study blocking diode resistance has been neglected.

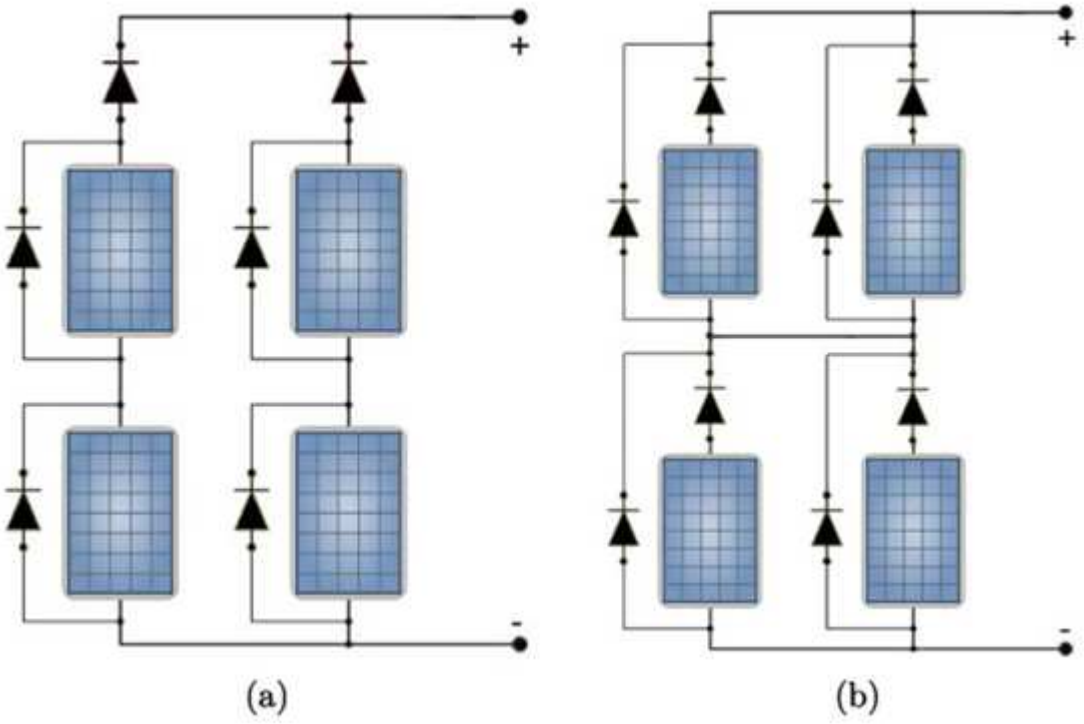

Figure 2.5: 2x2 PV array with bypass diodes across each PV module, and blocking diodes (a) in the top of each PV string within PV array connected in SP configuration, (b) across each PV module within PV array connected in TCT configuration.

2.4.4 PV module Simulation and GUI development using Matlab/Simulink software

The GUI is used to introduce the PV module where its parameters values are available from the manufacturer's datasheet and compute the two parameters R_s , R_p at STC. In addition, The GUI takes into account the effects of temperature, irradiation, shading, and diodes protection (bypass and blocking) [21].
In our case the PV module $MSX-60$ is taken as an example with the parameters values given in the Table.2.1.

The developed GUI allows us, also, to select the number of cells per bypass diode as shown in the Fig.2.7. Furthermore, selection of the bypass diode connection per number of PV cells can be chosen in the pop-up menu of the GUI whether one bypass

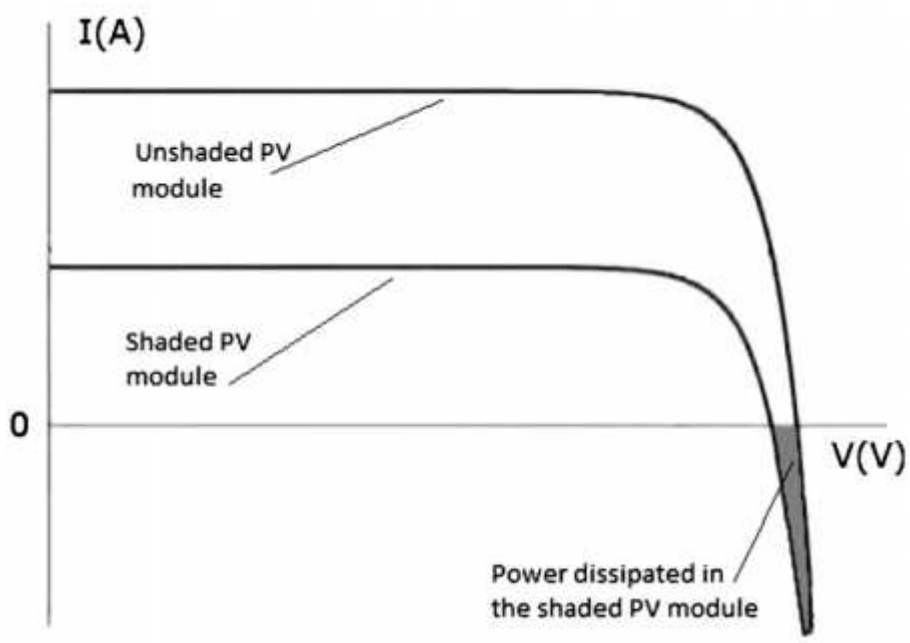

Figure 2.6: Impact of blocking diode on the (I-V) PV characteristic of two PV modules connected in parallel.

I_{sc}	3.8 A	K_v	$-80mV/^oC$
V_{oc}	21.1 V	K_i	$3m\%/^oC$
I_{mpp}	3.5 A	N_{cell}	36
V_{mpp}	17.1 V	P_{max}	58 W

Table 2.1: Parameters of MSX-60 PV module.

diode is for 36 cells, 18 cells or none.

The $I-V$ and $P-V$ curves for the example simulation case given in the GUI at temperature 25 ° C, with partial shading effect coefficients (1 K W/m2, 2/3 K W/m2) applied respectively to the first and second half group of PV cells (18 PV cells in this case) protected by separated bypass diode .

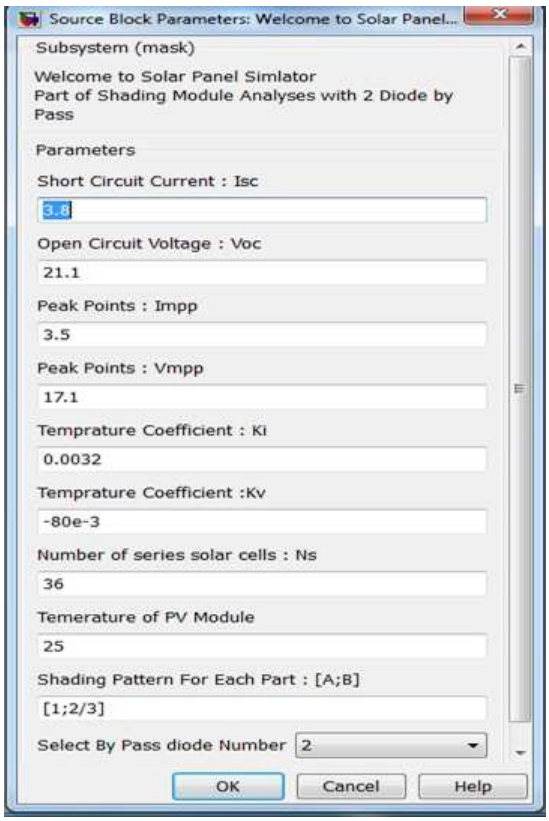

Figure 2.7: PV block input parameters window for MSX-60 PV module .

2.5 Characteristics of a partial shadow effect

The characterization of the partial shading effect is made by dividing it into four main part conditions, namely Short Wide (SW), Short Narrow (SN), Long Wide (LW), and Long Narrow (LN) as seen in the Fig.2.8(a). The shading conditions are defined based on the number of shaded columns (width) and shaded modules per column (length) Fig.2.9 [13].

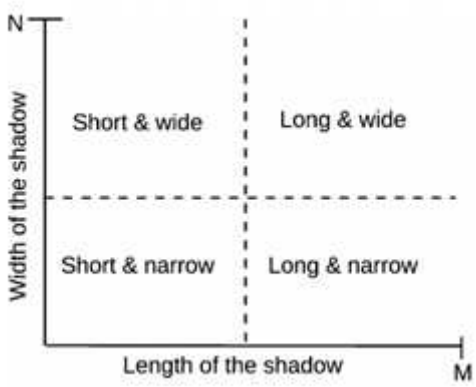

Figure 2.8: The four main shading pattern types .

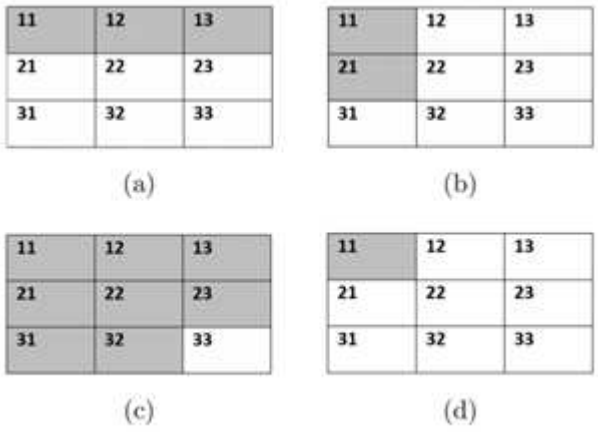

Figure 2.9: The shading type for 3x3 PV array. ((a) Short and Wide. (b) Narrow and Long. (c) Wide and Long. (d) Short and Narrow).

2.6 Impact of shaded PV modules arrangement on 3x3 PV array

The reduced power output is not related just to the partial shading area but much more to shading pattern [12]. Different shadow pattern, under four main types, is investigated in order to find the optimal relation between shaded modules locations and GMPP.

The simulation setup of 3x3 PV array for different shading pattern (Fig.2.9), is taken as an example to explore all shaded PV module arrangements and GMPP is calculated for each arrangement case.

The 3x3 PV array simulation setup is based on Matlab/Simulink built with nine separate PV modules, where each PV module has its own interactive graphic interface (GUI), as it was described in this chapter.

A PV array with two distinct groups is considered for all shading types. The first group is maintained at 100% shading (no illumination), while the remaining modules have full illumination, as it is described in Fig.2.9. Maximum power point (MPP) is extracted from the array at different shaded PV modules physical location or by another PV modules arrangement.

2.6.1 Short and Wide

GMPPs are extracted and investigated for all different locations of shaded PV modules in a 3x3 PV array for short and wide shading patterns as shown in Fig.2.9(a).

The Table.2.2 shows that regardless of the PV array arrangement, the shaded modules have three GMPPs values (346.7, 308.5 and 233.1 W). The GMPP is maximal when all shaded modules are in different rows, decreases when shaded modules are in the same row, and is the lowest for all other locations of shaded modules.

Nbre	Shaded modules	MPP	Nbre	Shaded modules	MPP
01	[11,21,31]	346,74	46	[21,22,33]	233,11
02	[11,21,12]	233,13	47	[21,32,13]	346,51
03	[11,21,22]	231,44	48	[21,32,23]	233,15
04	[11,21,32]	346,69	49	[21,32,33]	233,07
05	[11,21,13]	233,11	50	[21,13,23]	231,40
06	[11,21,23]	231,40	51	[21,13,33]	346,45
07	[11,21,33]	346,64	52	[21,23,33]	233,15
08	[11,21,33]	346,64	53	[21,23,33]	233,15
09	[11,31,12]	233,14	54	[31,12,22]	346,69
10	[11,31,12]	233,14	55	[31,12,22]	346,69
11	[11,31,22]	346,59	56	[31,12,32]	231,43
12	[11,31,32]	231,38	57	[31,12,13]	233,14
13	[11,31,13]	233,14	58	[31,12,23]	346,563
14	[11,31,23]	346,45	59	[31,12,33]	231,43
15	[11,31,33]	231,38	60	[31,22,32]	233,16
16	[11,12,22]	233,15	61	[31,22,13]	346,59
17	[11,12,22]	233,15	62	[31,22,13]	346,59
18	[11,12,32]	233,16	63	[31,22,23]	233,11
19	[11,12,13]	308,46	64	[31,22,33]	233,14
20	[11,12,23]	233,08	65	[31,32,13]	231,38
21	[11,12,33]	233,14	66	[31,32,23]	233,07
22	[11,22,32]	346,64	67	[31,32,33]	308,46

2.6.2 Narrow and Long

The simulations for the narrow and long type of shadow scenario on a 3x3 PV array, are shown in Fig.2.9(b). The corresponding GMPPs are summarized in Table.2.3. The simulations show two distinct GMPPs for some shaded PV module arrangements: 363.8 W and 316.2 W. The maximal value is obtained when all shaded modules are located in different rows; otherwise the GMPP is minimal (316.2 W).

2.6.3 Wide and Long

Table.2.4 lists the GMPP data for the Wide and Long pattern shadow type (Fig.2.9(c)). The GMPP is minimal (41.3 W) when the unshaded PV module is in the first row. For other arrangements the GMPP is maximal (41.7 W). For small 3x3 PV arrays the GMPPs remain almost identical for all possible arrangements, but for larger PV array

Nbre	Shaded modules	MPP	Nbre	Shaded modules	MPP
23	[11,22,13]	233,14	68	[31,13,23]	346,64
24	[11,22,23]	231,31	69	[31,13,33]	231,38
25	[11,22,33]	346,59	70	[31,23,33]	233,11
26	[11,32,13]	233,16	71	[12,22,32]	346,74
27	[11,32,23]	346,51	72	[12,22,13]	233,15
28	[11,32,33]	231,38	73	[12,22,23]	231,44
29	[11,13,23]	233,11	74	[12,22,33]	346,69
30	[11,13,33]	233,14	75	[12,32,13]	233,16
31	[11,23,33]	346,56	76	[12,32,23]	346,61
32	[21,31,12]	346,67	77	[12,32,33]	231,43
33	[21,31,22]	233,17	78	[12,13,23]	233,13
34	[21,31,32]	233,14	79	[12,13,33]	233,14
35	[21,31,13]	346,56	80	[12,23,33]	346,67
36	[21,31,23]	233,15	81	[22,32,13]	346,64
37	[21,31,33]	233,11	82	[22,32,23]	233,17
38	[21,12,22]	231,44	83	[22,32,33]	233,16
39	[21,12,32]	346,61	84	[22,13,23]	231,44
40	[21,12,13]	233,08	85	[22,13,33]	346,59
41	[21,12,23]	231,40	86	[22,23,33]	233,17
42	[21,12,33]	346,56	87	[32,13,23]	346,69
43	[21,22,32]	233,17	88	[32,13,33]	231,38
44	[21,22,13]	231,31	89	[32,23,33]	233,14
45	[21,22,23]	308,46	90	[13,23,33]	346,74

Table 2.2: part 01 and 02 : GMPPs at different shaded PV module location for Short and Wide shadow pattern type

the gap between GMPP values increases.

2.6.4 Short and Narrow

GMPP of shaded PV modules physical arrangements in a 3x3 PV array for Short and Narrow shadow patterns (Fig.2.9(d)) are listed in Table.2.5. Two distinct GMPPs are obtained; the smaller at 384.5 W occurs when the shaded PV modules are in the first row; for all other arrangement GMPP increases to 386.5 W. These results indicate that different shaded modules location have a small impact in PV array power production for small PV arrays. Future research will investigate the impact of the shaded PV modules arrangements for larger arrays.

Nbre	Shaded modules	MPP	Nbre	Shaded modules	MPP
1	[11,21]	363,88	19	[31,13]	363,81
2	[11,31]	363,81	20	[31,23]	365,39
3	[11,12]	316,24	21	[31,33]	316,24
4	[11,22]	363,79	22	[12,22]	363,90
5	[11,32]	363,83	23	[12,32]	363,87
6	[11,13]	316,24	24	[12,13]	316,24
7	[11,23]	363,46	25	[12,23]	363,79
8	[11,33]	363,81	26	[12,33]	363,85
9	[21,31]	365,52	27	[22,32]	365,54
10	[21,12]	363,79	28	[22,13]	363,79
11	[21,22]	316,24	29	[22,23]	316,24
12	[21,32]	365,46	30	[22,33]	365,48
13	[21,13]	363,68	31	[32,13]	363,83
14	[21,23]	316,24	32	[32,23]	365,46
15	[21,33]	365,39	33	[32,33]	316,24
16	[31,12]	363,85	34	[13,23]	363,88
17	[31,22]	365,48	35	[13,33]	363,81
18	[31,32]	316,24	36	[23,33]	365,52

Table 2.3: GMPPs at different shaded PV module location for Narrow and Long shadow pattern type.

Nbre	Unshaded modules	MPP
1	[11]	41,2569
2	[21]	41,6996
3	[31]	41,718
4	[12]	41,2944
5	[22]	41,7214
6	[32]	41,7285
7	[13]	41,2569
8	[23]	41,6996
9	[33]	41,718

Table 2.4: GMPPs at different shaded PV module location for Wide and Long shadow pattern type.

Nbre	shaded modules	MPP
1	[11]	384,4735
2	[21]	386,5805
3	[31]	386,6279
4	[12]	384,5215
5	[22]	386,6374
6	[32]	386,6557
7	[13]	384,4735
8	[23]	386,5805
9	[33]	386,6279

Table 2.5: GMPPs at different shaded PV module location for Short and Narrow shadow pattern type.

2.7 Conclusion

An overview of photovoltaic systems problem under no uniform irradiance was conducted to understand partial shading effect point of view from the PV cell to PV array. Characterizing the partial shading effect and dividing it into four main types is one of the result of this chapter. These results allow us to analyze the impact of the partial shading effect in the PV array efficiently.

Furthermore in this chapter, an overall of the hot spot phenomenal has been analyzed at different level of the PV system, pointing the important of the protection diodes in order to minimize the partial shading effect and avoiding the PV cells and modules damage.

A simulation at the end of this chapter proves that the shaded PV modules locations, within the PV array, have a direct impact in the PV power output production. In addition, the shaded PV module location and arrangements within PV array are related to the severity of the partial shading effect power loss. Thus, it is crucial to study and analyze the PV modules arrangement and configuration as an important way to minimize the partial shading effect. This necessary study and analysis is proposed in the next chapter.

CHAPTER 3

IMPACT OF PV CONNECTIONS, CONFIGURATIONS AND ARRANGEMENTS TO MINIMIZE THE PARTIAL SHADING EFFECT

3.1 Introduction

A PV array consists of individual PV modules electrically connected together to increase their power output. However, these connections can be changed within a PV array and so each new connection structure correspond to a new configuration .
The following chapter will study different type of PV array connections, configurations, and arrangements. We examine some of the important issues which arise as a result of partial shading effect especially power output reducing. Furthermore, it points the importance and difference between configurations in order to minimize the partial shading effect. As a result, a relationship between PV array configurations and the power output of PV system under partial shading is concluded during this chapter.

3.2 PV modules connections

PV arrays are built by connecting the PV module together in either parallel or series combinations to make larger arrays. This technique is the effective and simplest way to increase the PV array output by increasing both the voltage and current output. However, the types of the connection between PV modules determine the efficiency of the PV array configuration especially under particular requirements. The principles of how to connect multiple PV modules is discussed initially as follow:

3.2.1 PV modules in series connection

The connection in series is when the voltage of a PV array output is increased by connection the PV modules to another PV module accordingly to the Fig.3.1. In contrast, the current of the whole string is determined by the PV module that delivers the smallest current. Hence, the total current in a string within PV array is equal to the smallest current generated by one single PV module.
The I-V curve with blue color of the PV modules connected in series is shown in the Fig.3.2 .

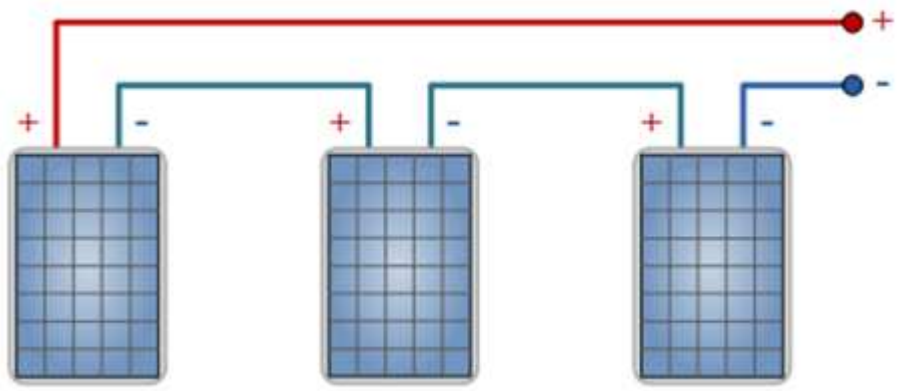

Figure 3.1: PV modules connected in series.

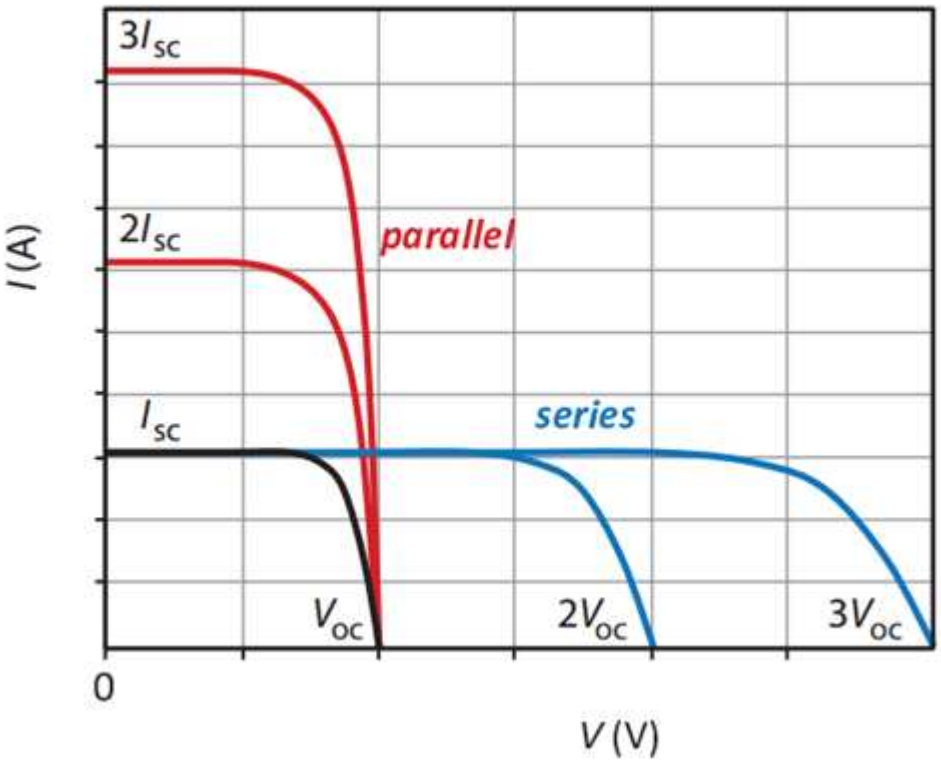

Figure 3.2: I-V characteristic curves of PV modules connected in series and parallel.

3.2.2 PV modules in parallel connection

The parallel connection between PV modules increases the current output of a PV array while the voltage is kept the same. Parallel connection is when the positives terminals of multiple modules are connected together and so, for all the negatives as illustrated in Fig.3.3. In the PV modules with parallel connections, the voltage is the same over all PV modules, while the currents of the PV modules add up, as illustrated in the I-V curve with red color as shown in the Fig.3.2. However, the high output current with low voltage in parallel connection will have to be properly conditioned to the required level by using suitable DC-DC converter.

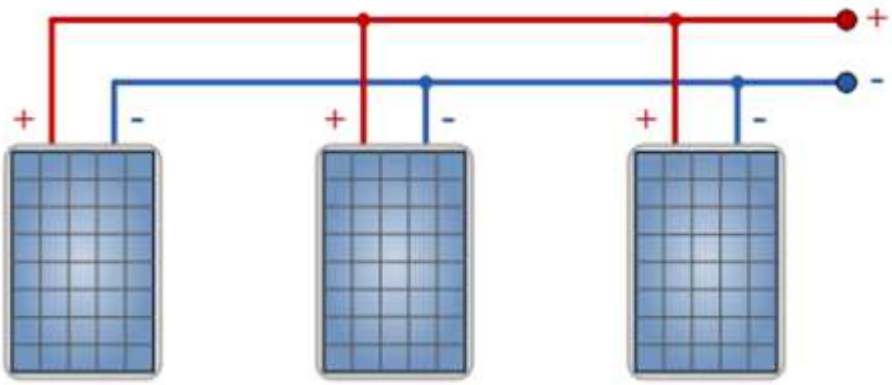

Figure 3.3: PV modules connected in parallel.

3.2.3 Series/ Parallel Combination between series and parallel connections

Different connection between PV modules within PV array can be made by combining the series and parallel connection, the simplest and the most known structure. However, in general the type of the connection is related to the applications. Beside, several groups of parallel-connected PV modules can be connected in series but for the PV cells within PV modules the things are complicated; this type of connection can

increase the current which needs cables with big sections, which this lead to increase the resistivity losses in the cables that connect the PV cells together.

3.3 Performance of Parallel and Series connection under partial shading condition

Series connection of PV modules within the PV array is essential to practically increase the PV array voltage output. A number of such strings are connected in parallel to get the requisite current PV array output. Besides, when PV modules, under partial shading condition are connected in series, the voltages still add, but the current is limited by the lowest current output of the shaded PV modules in series.
Theory and practice confirm that the effect of partial shading on a PV modules connected in parallel is less compared to series PV modules, although there is a decrease in the output current of the parallel PV modules [49]. Several studies had compared series and parallel connection of PV modules within PV array under different shaded conditions [50, 51]. It has shown that the parallel connection under partial shading condition is dominating series connection. So, the parallel connection is the best possible connection. The problem reside in high current and low voltage at the PV array output in parallel connection; thus, the system requires optimal use of PV modules interconnection and configuration.

3.4 Interconnection

Throughout all interconnection possibilities between PV modules in the PV array, the series, parallel, even other complicated connections can be manipulated easily, hence the importance of matrix connection conception.
Fig.3.4 shows the concept of connection matrix for a $3x3$ PV array; the connection in the 3x3 PV array refer practically to an ON/OFF switch in order to swap from any configuration to another at any time.

0	0	0	0	0	0	1	0	0	1	1	1	0	0	1	1	1	1	0	1	1	0	1	1
0	0	1	0	0	1	0	0	0	0	0	0	1	1	0	1	1	0	1	1	1	1	1	1

Table 3.1: Connection matrices values for 3x3 PV array to swap from to any PV array configurations.

The Table.3.1 present the connection matrix composed by ones and zeros which represents (ON/OFF) connections for $3x3$ PV array respectively. The connections in the PV array can be realized by switch to swap from ON/OFF as shown in the Fig .3.4. In general, by combining different ON/OFF switching matrices, different PV array configuration may be obtained. These connections possibilities between PV modules within the PV array, given in the Table .3.1. These configurations will be discussed in more detail in the coming sections.

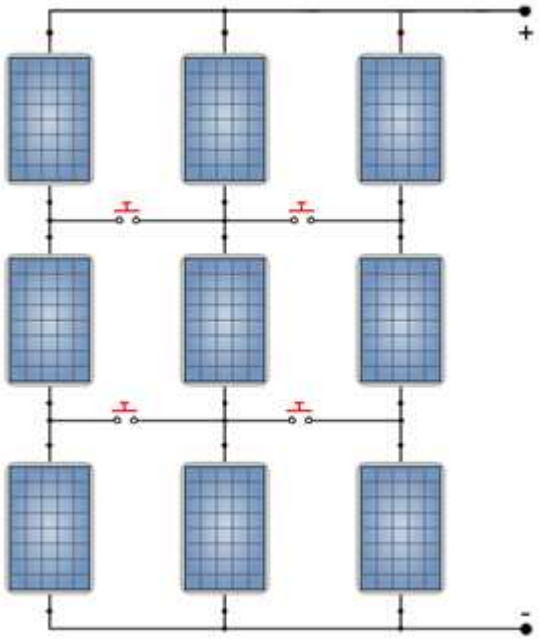

Figure 3.4: Visual concept of a connection matrix over a $3x3$ PV array.

3.5 Study of different configuration and arrangements under partial shading effect

The partial Shading effect influences directly the PV module/array performance and output power. Since it is usually not possible to avoid partial shading due to clouds, dirt, etc. [52]. It is then, important to investigate the most favorable relationship between shading pattern type, interconnection, configuration and PV module arrangement in order to increase PV array power yield and eliminate multiple peaks in the P-V characteristic [50]. Use of an optimal interconnection, conventional configuration, Electrical Array Reconfiguration and PV array physical arrangement are analyzed and investigated in order to determined which one is particularly suitable for minimizing the partial shading effects on the PV array [1]. Furthermore, power losses as well as PV degradation can also be reduced by adding bypass and blocking diode [53].

In the following sections, the different configuration approaches proposed in the literature will be discussed.

3.5.1 Conventional PV configurations

The PV arrays consist usually of PV modules connection in serie-parrallel (SP) to fit power converter specifications. However, there is three more main configurations : bridge-link (BL), honey comb (HC) and total cross tied (TCT) [1] as seen in Fig.3.5.

In Total cross-tied (TCT) configurations as seen Fig.3.5 (d), PV modules are first parallel connected together so that voltages are equal and currents are added. Many of these parallel PV modules groups are then connected in series. Whereas under the partial shading conditions SP and TCT modules connection provide the same power value, the TCT topology reduces the overall partial shading effect [26]. Several works show that TCT configuration minimizes the partial shading effect losses and has the highest performance under the most cases of partial shading conditions compared to other PV configurations [54], .

The SP configuration has the lowest performance under partial shading conditions while BL and HC configuration have medium performances. Theirs connections for a 3x3 PV array are given in Fig.3.5 [26, 55]. Thus, the PV array power output is related to the performance of these configurations. Even though the Bridge-link (BL) configuration, in Fig. 3.5 (b), is about half of the interconnections of the TCT configuration are avoided, so reducing cable losses and wiring installation. But, in larger installations, the TCT arrangement can be easier to wire because of the simplicity of the pattern. Advantages shown by both TCT and BL configurations have been combined in the Honey Comb (HC) configuration Fig.3.5 (c). Besides of this, many convenient interconnection configurations have been developed.so far the most exploited solutions are TCT and SP configurations [55]. Many works prove that TCT configuration has the highest performance in term of PV array power output, especially under partial shading effect [26].

It is Important to note that the PV model of the PV cell/module can be used to represent the $I-V$ and $P-V$ characteristic of a practical PV array. In order to avoid using complicated mathematics equations for each configuration interconnection between each PV module, blocking and bypass diodes protection are used.

3.5.2 The Electrical Array Reconfiguration (EAR)

The approach of EAR is to change the electrical connection of PV module within a PV array according to shading pattern in order to minimize PV array power loss. The EAR controller needs mainly switching matrix and sensors to do this adaptation [15, 56] as resumed by the flow chart in the Fig.3.6.

The reconfiguration basic principle strategy of relocating and connecting PV modules, the description is in Fig.3.7(a). This is done, in such a way that the sum of irradiances at each row are equal as seen in the Fig.3.7(b) for a 3x3 PV array [56]. Furthermore, there are many possible configurations with different developed control algorithm that determine how and when to adaptively turn the switches to ON or OFF.

The researchers have developed several approaches for adaptive reconfiguration of

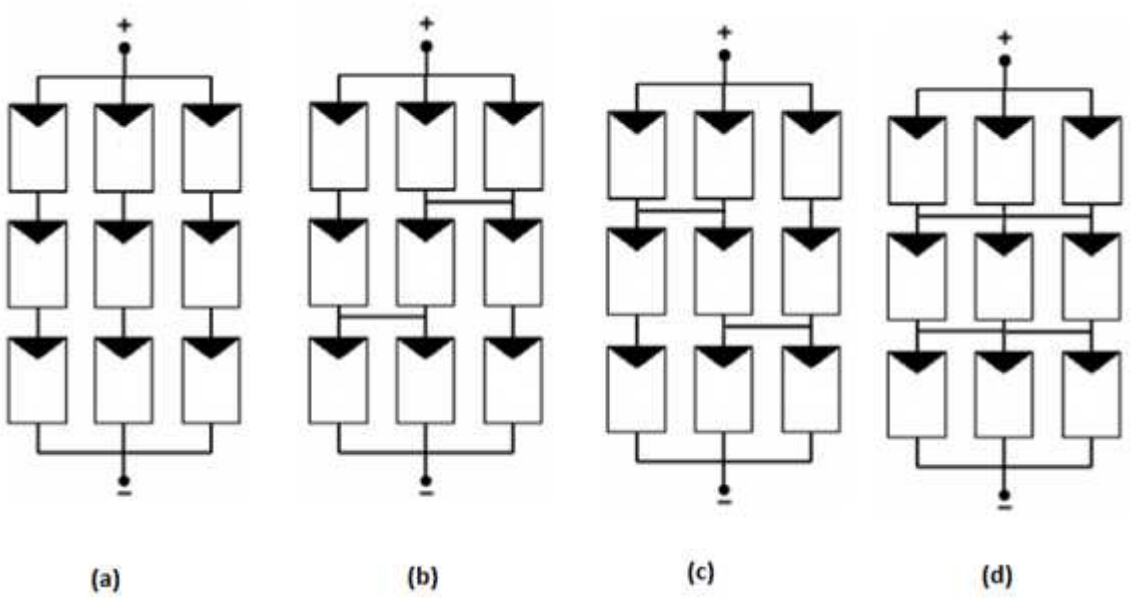

Figure 3.5: PV array configurations (a) SP, (b) BL, (c) HC and (d) TCT.

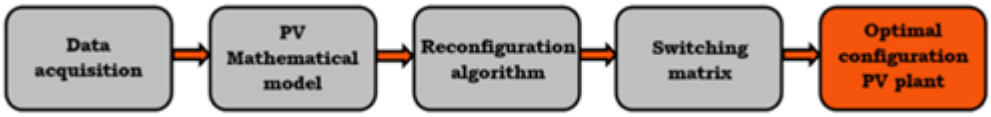

Figure 3.6: Flow chart of the AER configuration controller [1].

PV arrays [50, 57]. They proposed methods that require different switches and sensors which can be either simple or complicated implementation in the real time control algorithm. This becomes an adaptive algorithms to reconfigure connections within PV arrays in real time, especially under partial shading conditions, in order to maximize PV array power output and minimize the partial shading effect.

Another approach of EAR proposes to connect a matrix switches between a TCT fixed PV array and a solar adaptive bank as seen in Fig.3.8 [58]. Thus a new approach of a control algorithm reconfiguration to produce an optimal power, is needed. In addition the implementation of such algorithm in real-time is needed as well. This new approach makes EAR more complicated and expensive.

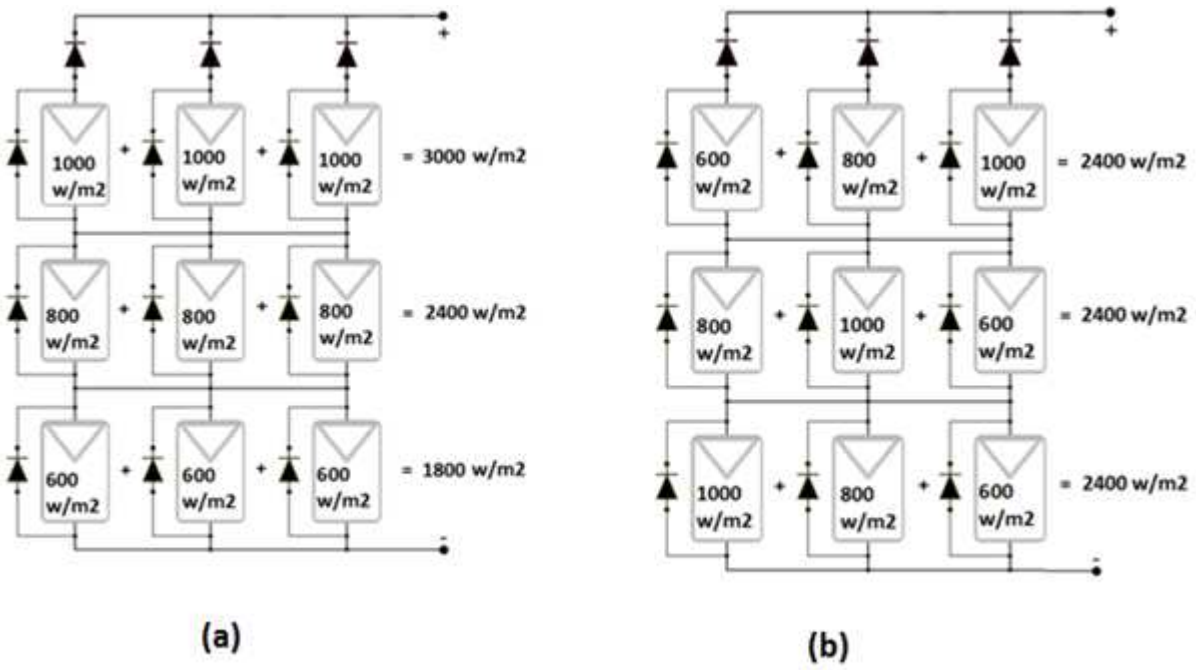

Figure 3.7: Principle of the reconfiguration strategy. (a) Initial configuration. (b) Final configuration.

3.5.3 PV array physical arrangement based on a TCT configuration

The physical PV array arrangement is based on the TCT configuration. However, the initial physical PV array arrangement is changed with the same electrical connections [58]. In order to disperse as much as possible the shading pattern uniformly over the entire PV array. Su Do Ku arrangement has been proposed in the paper [59]. This arrangement, which is shown in in Fig.3.9, is taken as an example in our work.

The principle of a Su Do Ku arrangement is to alter the row of each PV module position in a 9X9 PV array in order to improve the PV array power output under partial shading conditions. The column number remains the same as in the TCT configuration. The PV modules remain in the same column as in the TCT configuration. However, theirs positions within the PV array column are changed in such a way that only the row of the PV modules physical positions are changed. The electrical

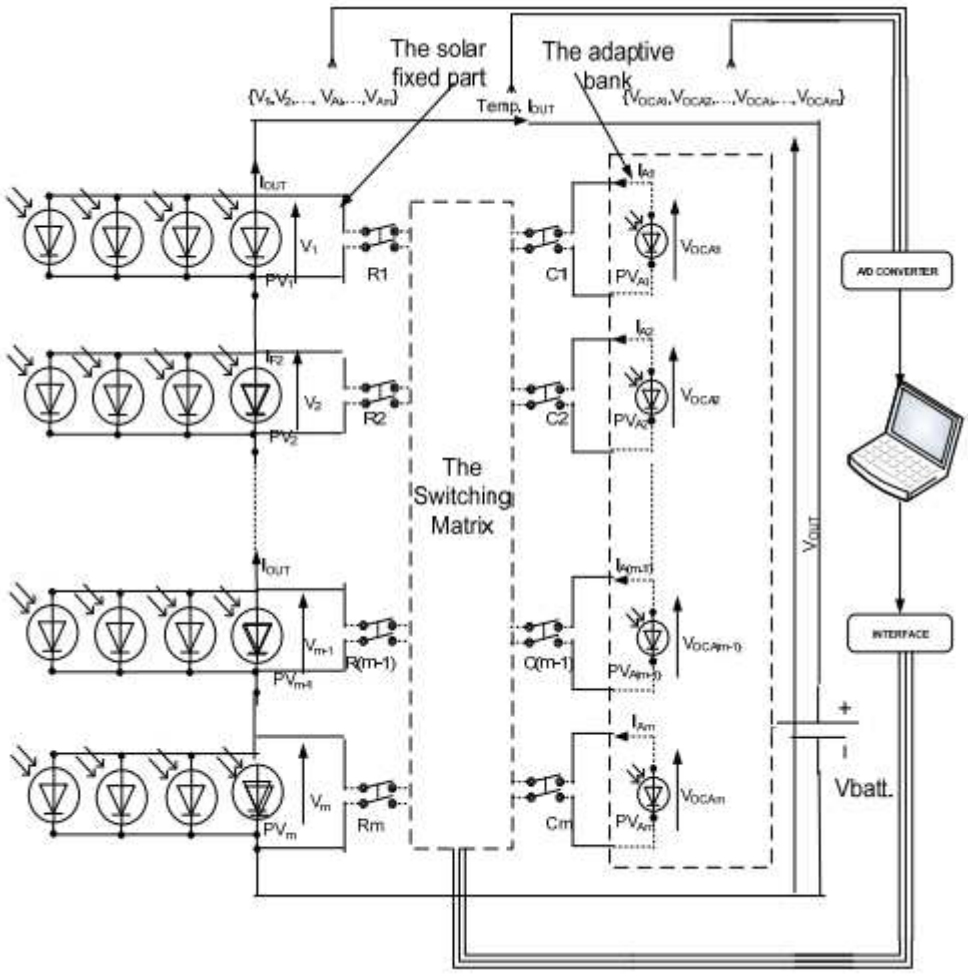

Figure 3.8: Practical circuit of the new approach of AER with adaptive bank.

connections of the PV modules remain unchanged as in a normal TCT configuration; beside of this only the physical positions within PV array column of the PV modules are changed. The PV module in the 3rd row and 2nd column is physically relocated to the 4th row with the same initial column (2nd); besides, as the electrical connection is still unchanged, it means that the PV module remains electrically connected to the PV modules in the (2rd row , 2nd column) and the (4rd row , 2nd column) respectively.

The PV module physical relocation within PV array given by Su Do Ku arrangement insures the distribution of the shaded PV modules over the entire PV array. This PV modules distribution aims to reduce correlation between shaded modules in order to

minimize the partial shading effect.

It is important to note that Su Do Ku or whatever other arrangement, with the same principle is considered as a fixed arrangement and not as the EAR dynamical changing. This means that the arrangement of the PV array remains the same once it is configured and relocated for all shading patterns (static) at any time.

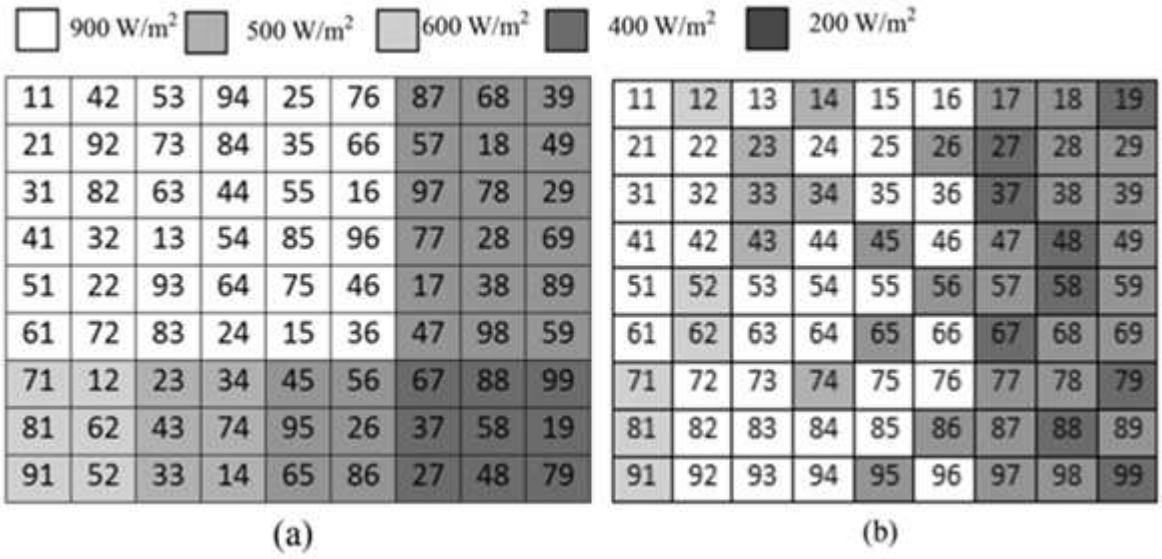

Figure 3.9: 9x9 PV array under partial shading condition with different irradiance level. (a) The initial arrangement. (b) Su Do Ku arrangement.

3.6 Comparisons and summary of PV array configurations and arrangements

The conventional configurations are the cheapest techniques that can overcome the partial shading effect compare to the EAR configuration as shown in the Table.3.2, based on the previous explications. However, these conventional configurations cannot eliminate the local peaks exhibitions on the P-V characteristic. As a consequence, the tracking by the conventional MPPT of the PV array power maximum output can be trapped easily on one of these local peaks LMPPs.

	Cost	Complexity	eliminate LMPPs	Power losses
Conventional Configurations	Cheap	Low	No	Vary
Electrical Array Reconfiguration	Expensive	Very high	Yes	Low
PV array physical Arrangements	Cheap	Low	Yes	Low

Table 3.2: PV array configurations comparison summary.

On the other hand, the EAR use a controllable switching matrix and sensors that make it complicated and expensive compared to PV array arrangement and conventional configurations.

The PV array physical arrangements are cheap techniques since they don't need a sensors and controller. However, these arrangements techniques give better performance to minimize shading effect power loss and eliminate the LMPPs exhibition on the P-V curve characteristics. Thus, the importance to develop PV array arrangement that can not only overcome the partial shading effect efficiency but also the cost stays low.

The reduced power output and the LMPPs exhibition are not related just to the partial shading effect but much more to shading pattern [60]. The PV array arrangement and Electrical Array Reconfiguration (EAR) has a real impact to eliminate these LMPPs under different partial shading types and patterns. Many arrangements have been proposed such as Su do Ku and others shows the efficiency of such a technique to improve the PV array yield and eliminate the exhibition of LMPPs on the P-V characteristic [51, 61] as seen in the Fig.3.10.

3.7 Conclusion

A discussion on the research contribution for different connections, configurations and arrangement, has been discussed. A Weakness and strength, in term of efficiency, complication and cost, for each one of these PV configurations are deeply investigated.

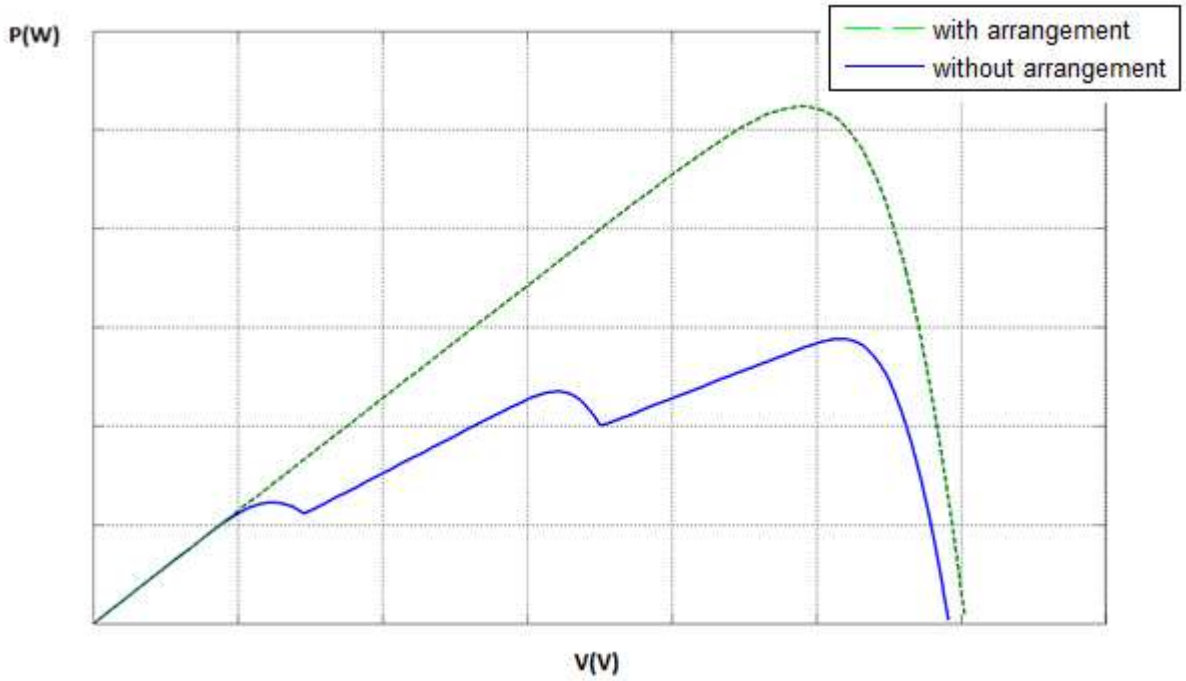

Figure 3.10: P-V characteristic of PV array with and without arrangement.

This state of art, given in this work, points the importance of the PV array arrangements compared to other configurations. The PV array arrangements can avoid the local maximum power points and maximizes the PV array power output even under partial shading conditions efficiently and with the lowest cost.

It is important to develop a new PV arrangement in order to improve the existent techniques under severe partial shading condition; this is the main objective of the next chapter.

CHAPTER 4

NEW SHIFTED PV ARRAY ARRANGEMENTS WITH COMPARISON

4.1 Introduction

The previous chapters prove that partial shading effect losses are dependent on the shading pattern and the relative positions of shaded modules within the PV array. In an earlier proposed PV array arrangements, the power generation is enhanced by changing the physical position of the PV modules base on TCT configuration, for our work Su Do Ku arrangement is taken as an example in order to point the efficiency of our proposed arrangements via the existing works.
The improvement in the yield energy in the proposed PV array arrangement is presented under different partial shading conditions with details further in this chapter. The results of GMPP are compared with existing and recent arrangement PV array configurations.

4.2 New physical PV array arrangement

The aim of the new proposed physical PV array arrangement connected in TCT is to enhance the GMPP by mitigating the shading effect and minimizing the variation between P-V characteristic curve peaks. To do this, we changed the initial physical location of the PV modules within PV array as shown in Fig.4.1(a),(d) to the a new PV array arrangement as given in Figs.4.1(b),(e) in order to improve the initial TCT configuration arrangement, the Figs.4.1(b),(e) show how the changes are implemented in each of the columns of the modified TCT (M-TCT) PV array arrangement. At the same time, we kept the initial electrical connections between PV modules unchanged. Therefore, the previously presented equations are still applicable for all the following computing.

The position shifting efficiency of the PV modules within PV array are studied through an example of 2x2 and 3x3 PV array as shown Fig.4.2. The impact of a cloud shadow across a 2x2 and a 3x3 PV array with two PV array configurations under the same cloud shading pattern: M-TCT and M-TCT with shifting, are illustrated in the

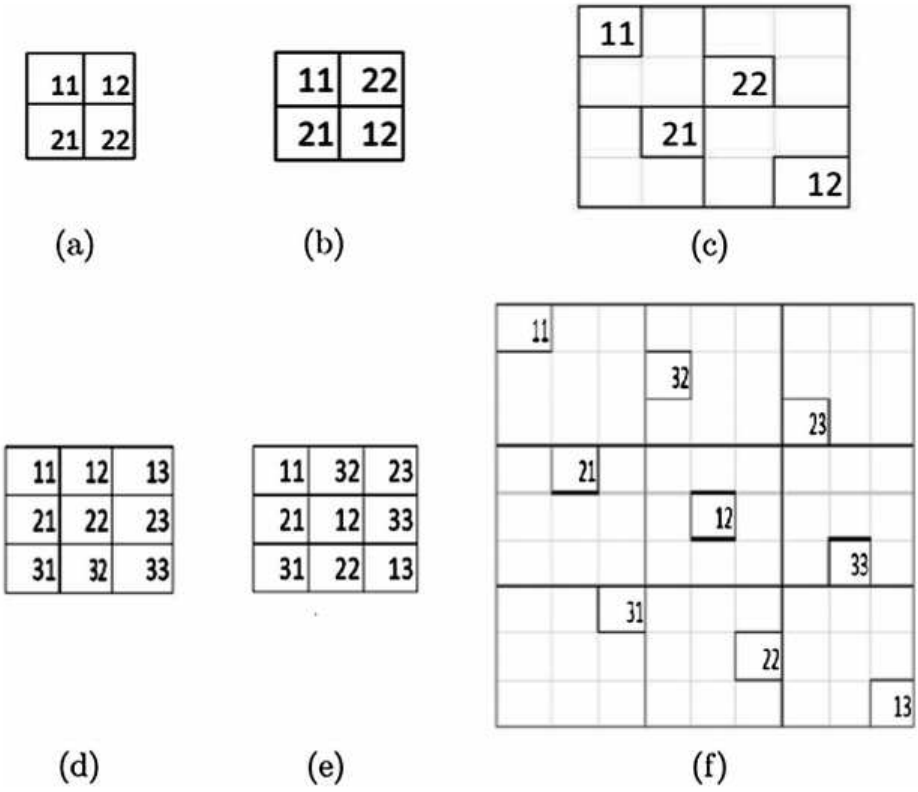

Figure 4.1: 2x2 PV array: (a) TCT. (b) Modified TCT arrangement. (c) Modified TCT with shifting . 3x3 PV array: (d) TCT. (e) Modified TCT arrangement. (f) Modified TCT with shifting.

Fig.4.2. To improve the PV array power output, the shifting procedure is applied. The GMPPs' of the 2x2 and a 3x3 PV array power output values for these configurations are given in the Table.4.1. In addition, the SP and TCT configuration power output are also taken into account in this table in order to compare all their performances. In other words, Table.4.1 compares the power output performances of these configurations with the SP and TCT ones.

Introducing the shifting to the modified TCT (M-TCT) allows to decrease the correlation between shaded PV modules and shadow patterns. The idea is to create an empty array (4X4/9X9) divided in equal sub-arrays (2X2/3X3) and distribute its PV modules in such way that it will not be at the same row and column as shown in Fig.4.1.(c),(f).

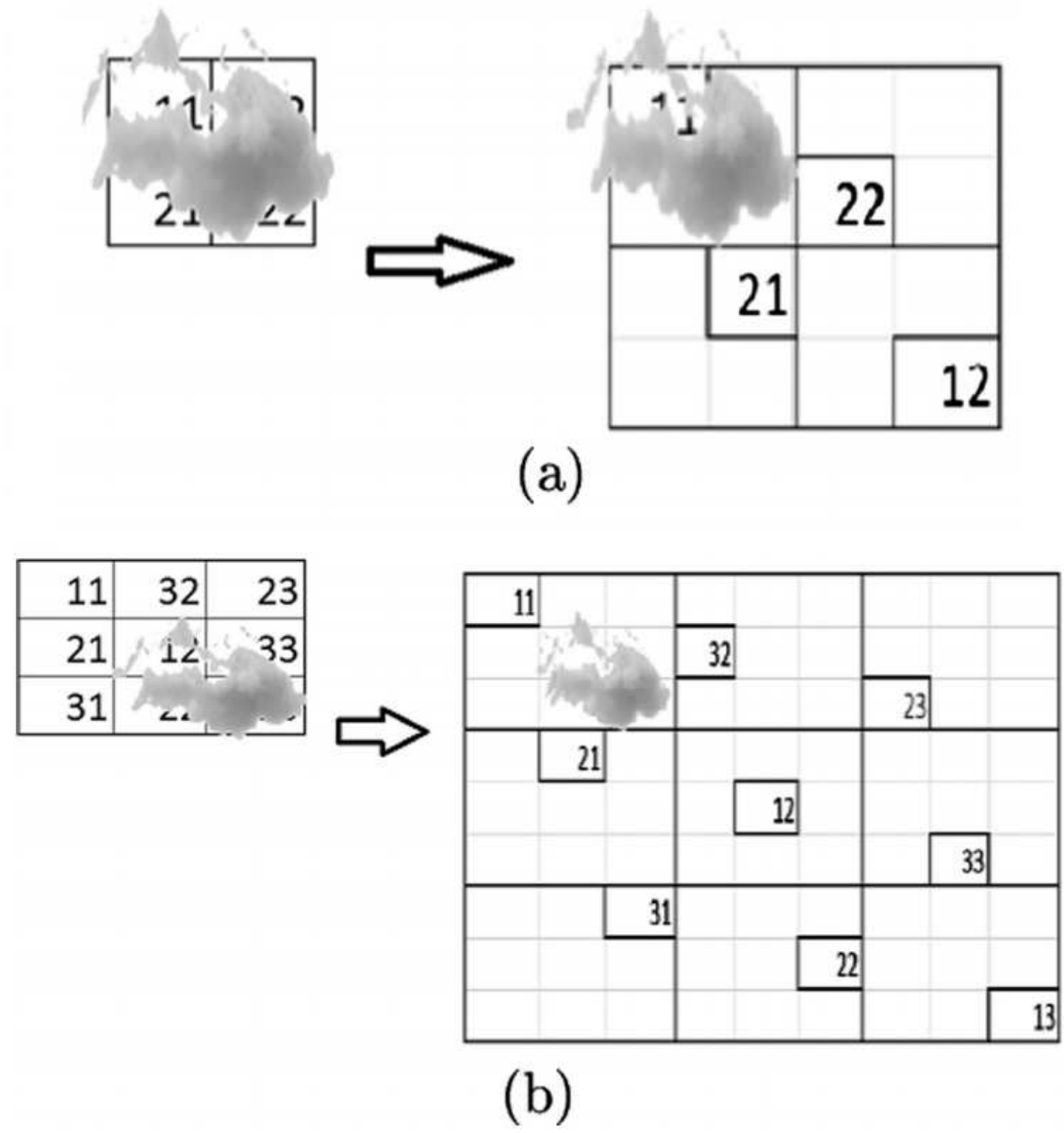

Figure 4.2: M-TCT arrangement with and without shifting: (a) 2x2 PV array; (b) 3x3 PV array.

	GMPP with comparison to unshaded PV Array			
	2x2 PV array		3x3 PV array	
	GMPP(W)	% GMPP	GMPP(W)	% GMPP
SP	0	0 %	174.60	33.33 %
TCT	0	0 %	185.33	35.38 %
M-TCT	0	0 %	215.74	41.19 %
M-TCT with Shifting	124.36	54.35%	523.80	100 %

Table 4.1: GMPP of different proposed configurations under shading for 2x2 and 3x3 PV array.

Since all PV modules of the 2x2 array are shaded as shown in Fig.4.2(a), the array does not produce any power with the SP, TCT and M-TCT configurations. However, the application of the shifting to the M-TCT increase the power output by 54%.
Table.4.1 shows also that for a shaded 3x3 PV array Fig.4.2(b), GMPP with these configurations attain only around 35% with STC, while by applying the shifting procedure to the TCT modified configuration, the GMPP of a 2x2 PV array increases from zero to about 54%, and 100% of GMPP is achieved for the 3x3 PV array, see the Table.4.1.

The major contribution of this proposed arrangement with shifting is to increase the space gap between adjacent PV modules as much as possible in different columns and rows in order to minimize the impact of the partial shading effect.
The weakness, of the M-TCT arrangement with shifting, is the wasted space shown in Fig.4.1. (c), (f). To resolve this problem, we fill up the extra space with PV modules from separate PV sub-arrays (from A to I) as shown in Fig.4.3. (b); we arrange this nine PV sub-arrays by changing their column, row, and even their position, in such a way that we put just one PV module of each PV sub-array on the selected 3x3 PV sub-array which is in the 9x9 PV array Fig.4.3. (a). As an example, the black highlighted PV modules of Sub array [A] are distributed all around the 9X9 array Fig.4.3. (a) which is the same thing for all other PV sub array.
We call this new proposed arrangement shift modified TCT (S-M-TCT), Fig.4.3.(a). Its

electrical connection is shown in Fig.4.3.(b). The purpose of S-M-TCT is to mitigate partial shading effects on the PV array by minimizing the correlation between shading patterns and the mismatch losses in the PV array. Besides, the blocking diode insertion for each PV module in the S-M-TCT arrangement has a real impact to increase its efficacy compared to other arrangements and configurations that do not use them or use just one at the top of the PV string. In addition, we need to make sure that the blocking diode has a very small resistance to minimize its consumption especially at uniform irradiance.

Fig.4.3.(c) shows the new proposed arrangement by connecting the sub-array of M-S-TCT arrangement in a parallel connection (parallel M-S-TCT). In this way, we can mitigate the shading effect and reduce the bypass diodes power dissipation.

4.3 The proposed PV arrangement: results and discussion

The efficiency of the proposed PV array arrangement is analyzed and compared with other configurations under different shading patterns. Their performances are shown thru the GMPP and how it minimizes the numbers of peaks on P-V characteristics curves.

Matlab/Simulink simulation tool is used to evaluate the PV arrangement performances.A PV array with two distinct groups is considered. The first group is completely shaded (no illumination); while the remaining modules have full illumination 1000 W/m^2, as it is observed for a distinct shading type shown below .

The GMPP P-V curves characteristics of the following PV array configurations: Parallel S-M-TCT, S-MTCT+BLK (S-M-TCT with the blocking diodes connected to each PV modules), S-M-TCT, Su Do Ku, TCT and SP under different shading pattern are shown respectively in Table.4.2 and Figs.4.4-4.13. For simplicity, we plot all the PV characteristics curves on the same graph and display their GMPP values in a separate table for each shadow pattern and scenario. The results are discussed as bellow:

11[A]	32[B]	23[C]	22[G]	13[H]	31[I]	33[D]	21[E]	12[F]
21[D]	12[E]	33[F]	32[A]	23[B]	11 [C]	13[G]	31[H]	22[I]
31[G]	22[H]	13[I]	12[D]	33[E]	21[F]	23[A]	11[B]	32[C]
33[C]	21[A]	12[B]	11[I]	32[G]	23[H]	22[F]	13[D]	31[E]
13[F]	31[D]	22[E]	21[C]	12[A]	33[B]	32[I]	23[G]	11[H]
23[I]	11[G]	32[H]	31[F]	22[D]	13[E]	12[C]	33[A]	21[B]
22[B]	13[C]	31[A]	33[H]	21[I]	12[G]	11[E]	32[F]	23[D]
32[E]	23[F]	11[D]	13[B]	31 [C]	22[A]	21[H]	12[I]	33[G]
12[H]	33[I]	21[G]	23[E]	11[F]	32[D]	31[B]	22[C]	13[A]

(a)

11[A]	32[A]	23[A]	11[H]	32[H]	23[H]	32[F]	23[F]	11[F]
21[A]	12[A]	33[A]	21[H]	12[H]	33[H]	12[F]	33[F]	21[F]
31[A]	22[A]	13[A]	31[H]	22[H]	13[H]	22[F]	13[F]	31[F]
23[D]	11[D]	32[D]	32[B]	23[B]	11[B]	23[I]	11[I]	32[I]
33[D]	21[D]	12[D]	12[B]	33[B]	21[B]	33[I]	21[I]	12[I]
13[D]	31[D]	22[D]	22[B]	13[B]	31[B]	13[I]	31[I]	22[I]
32[G]	23[G]	11[G]	23[E]	11[E]	32[E]	11[C]	32[C]	23[C]
12[G]	33[G]	21[G]	33[E]	21[E]	12[E]	21[C]	12[C]	33[C]
22[G]	13[G]	31[G]	13[E]	31[E]	22[E]	31[C]	22[C]	13[C]

(b)

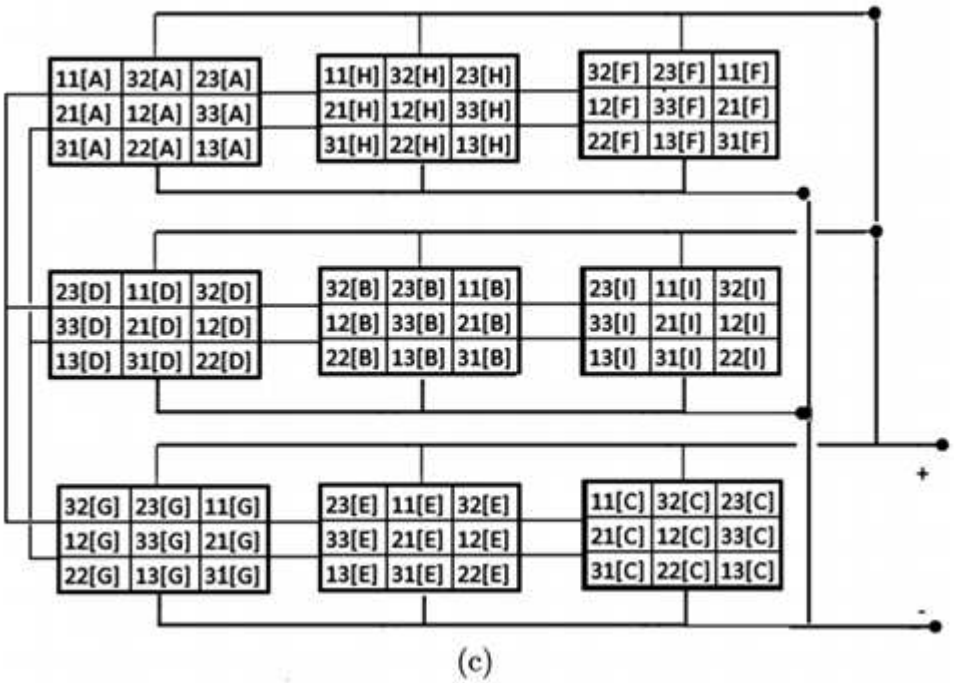

(c)

Figure 4.3: a). Physical location of S-M-TCT arrangement . b). Electrical connection of S-M-TCT arrangement .c). Electrical connection of parallel S-M-TCT arrangement.

4.3.1 Short and Narrow

The Short and Narrow shading pattern and physical S-M-TCT arrangement is depicted in Fig.4.4(a); the electrical connection to disperse the shading pattern for S-M-TCT and Parallel S-M-TCT are shown respectively in Fig.4.4.(b), Fig.4.4.(c).

11[A]	32[B]	23[C]	22[G]	13[H]	31[I]	33[D]	21[E]	12[F]
21[D]	12[E]	33[F]	32[A]	23[B]	11[C]	13[G]	31[H]	22[I]
31[G]	22[H]	13[I]	12[D]	33[E]	21[F]	23[A]	11[B]	32[C]
33[C]	21[A]	12[B]	11[I]	32[G]	23[H]	22[F]	13[D]	31[E]
13[F]	31[D]	22[E]	21[C]	12[A]	33[B]	32[I]	23[G]	11[H]
23[I]	11[G]	32[H]	31[F]	22[D]	13[E]	12[C]	33[A]	21[B]
22[B]	13[C]	31[A]	33[H]	21[I]	12[G]	11[E]	32[F]	23[D]
32[E]	23[F]	11[D]	13[B]	31 [C]	22[A]	21[H]	12[I]	33[G]
12[H]	33[I]	21[G]	23[E]	11[F]	32[D]	31[B]	22[C]	13[A]

(a)

11[A]	32[A]	23[A]	11[H]	32[H]	23[H]	32[F]	23[F]	11[F]
21[A]	12[A]	33[A]	21[H]	12[H]	33[H]	12[F]	33[F]	21[F]
31[A]	22[A]	13[A]	31[H]	22[H]	13[H]	22[F]	13[F]	31[F]
23[D]	11[D]	32[D]	32[B]	23[B]	11[B]	23[I]	11[I]	32[I]
33[D]	21[D]	12[D]	12[B]	33[B]	21[B]	33[I]	21[I]	12[I]
13[D]	31[D]	22[D]	22[B]	13[B]	31[B]	13[I]	31[I]	22[I]
32[G]	23[G]	11[G]	23[E]	11[E]	32[E]	11[C]	32[C]	23[C]
12[G]	33[G]	21[G]	33[E]	21[E]	12[E]	21[C]	12[C]	33[C]
22[G]	13[G]	31[G]	13[E]	31[E]	22[E]	31[C]	22[C]	13[C]

(b)

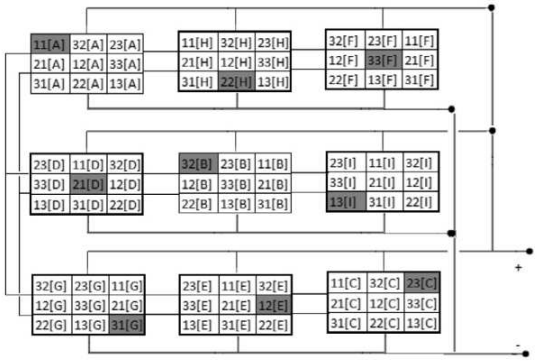

(c)

Figure 4.4: Short and Narrow shading pattern: (a) S-M-TCT physical arrangement; (b) S-M-TCT electrical connection; (c) // S-M-TCT electrical connection.

All S-M-TCT have an important impact to enhance the P-V curve showing just one peak MPP as shown in the Fig.4.5 . Since S-M-TCT changes the PV modules arrangement within PV array in such way that the generated current is the same for different columns and even the same for rows in the case of TCT configuration. The S-M-TCT with blocking diode and the parallel S-M-TCT have the highest GMPP with

just one peak on the P-V characteristic curve. On the other hand, the Su Do Ku arrangement has one MPP peak but the power generation is lower than the other S-M-TCT arrangement. Besides, TCT, SP configurations give the lowest GMPP with multiple peaks in the P-V characteristic curve.

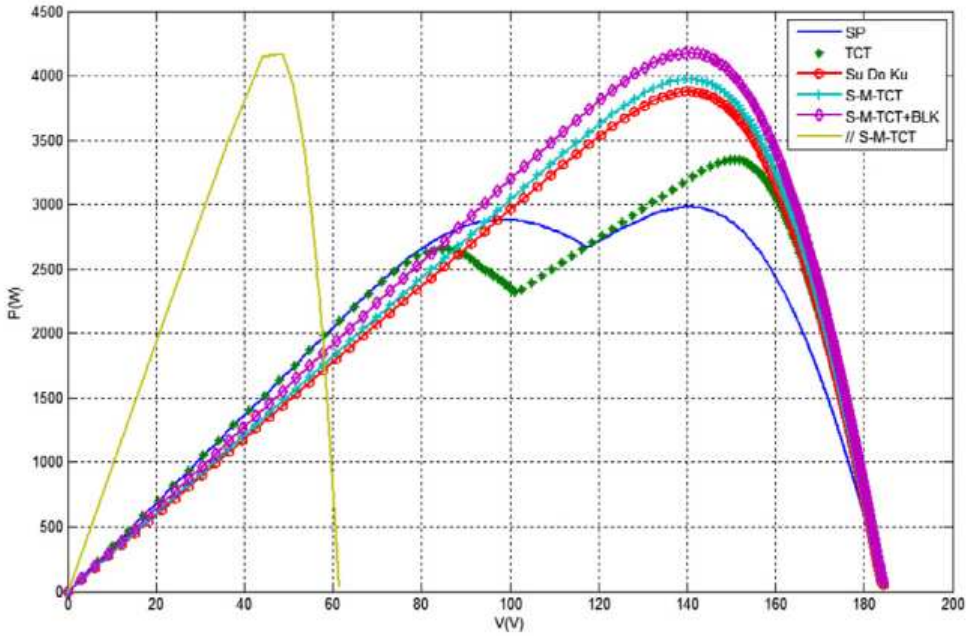

Figure 4.5: The P-V characteristics of different PV configuration of Short and Narrow shading pattern.

4.3.2 Narrow and Long

In this shading pattern case Fig.4.6 (a), Table.4.2 shows that GMPP power output generation of both //S-M-TCT and S-M-TCT+BLK proposed arrangement Fig.4.6(b),(c) has a major improvement over the SP, TCT and slightly over Su Do Ku and S-M-TCT. These P-V curves show that the S-M-TCT has a better performance to minimize shading pattern effect with a higher GMPP compared to Su Do Ku arrangement. We notice that there is just one MPP peak on the P-V characteristic curve for all proposed S-M-TCT and Su Do Ku arrangement, Fig.4.7. Beside of that, a small peak at the

begging of the P-V curve, shown in Fig.4.7 for the S-P and TCT configuration are noted; therefore the classic MPPT can be trapped easily at one of the LMPPs by using such configurations.

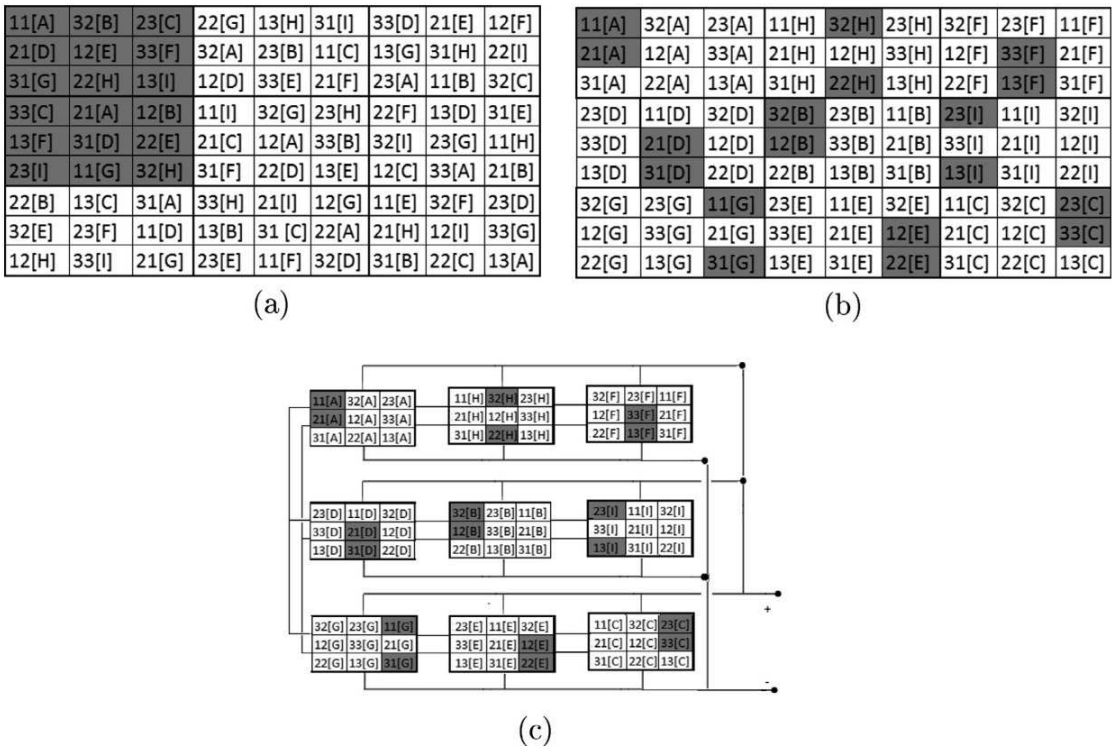

Figure 4.6: Narrow and Long shading pattern: (a) S-M-TCT physical arrangement; (b) S-M-TCT electrical connection; (c) // S-M-TCT electrical connection.

4.3.3 Short and Wide

The PV array power output, of the proposed physical PV array arrangement, Fig.4.8(b),(c) were also superior compared to other PV configuration without showing LMPP for this shading pattern, Fig.4.8(a), as shown in the Fig.4.9. The GMPP efficiencies of //S-M-TCT or S-M-TCT+BLK arrangements compared to SP, TCT, Su Do Ku, S-M-TCT are respectively as follows 19.73%, 19.73%,5% and 4.22%. These percentages calculation are based in Table.4.2.

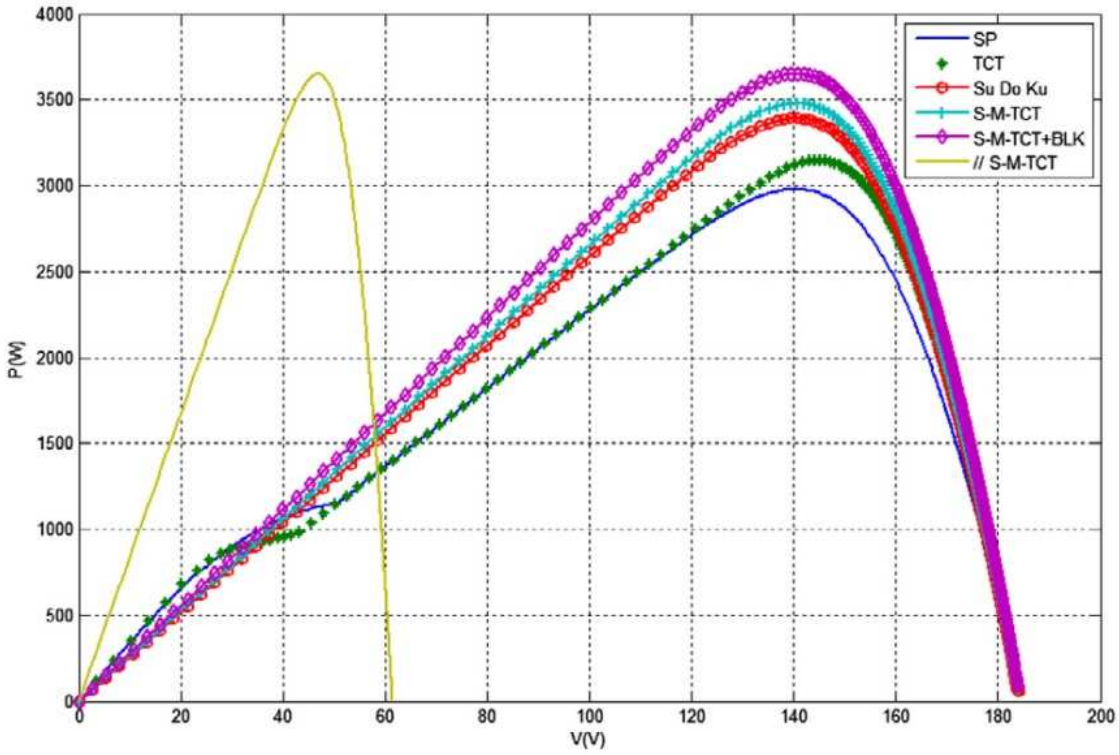

Figure 4.7: The P-V characteristics of different PV configuration of Narrow and Long shading pattern.

4.3.4 Wide and Long

In the case of a wide and long shading pattern as seen in the Fig.4.10(a) the shadow is distributed uniformly over the entire PV array by the proposed arrangement as shown in Fig.4.10(b),(c). The S-M-TCT and Su Do Ku arrangement still have the highest GMPP compared to other configurations Fig.4.11. In addition, the P-V curve in the Fig.4.11 shows the nonexistence of LMPP for all presented configurations for this shading pattern.

11[A]	32[B]	23[C]	22[G]	13[H]	31[I]	33[D]	21[E]	12[F]
21[D]	12[E]	33[F]	32[A]	23[B]	11[C]	13[G]	31[H]	22[I]
31[G]	22[H]	13[I]	12[D]	33[E]	21[F]	23[A]	11[B]	32[C]
33[C]	21[A]	12[B]	11[I]	32[G]	23[H]	22[F]	13[D]	31[E]
13[F]	31[D]	22[E]	21[C]	12[A]	33[B]	32[I]	23[G]	11[H]
23[I]	11[G]	32[H]	31[F]	22[D]	13[E]	12[C]	33[A]	21[B]
22[B]	13[C]	31[A]	33[H]	21[I]	12[G]	11[E]	32[F]	23[D]
32[E]	23[F]	11[D]	13[B]	31 [C]	22[A]	21[H]	12[I]	33[G]
12[H]	33[I]	21[G]	23[E]	11[F]	32[D]	31[B]	22[C]	13[A]

(a)

11[A]	32[A]	23[A]	11[H]	32[H]	23[H]	32[F]	23[F]	11[F]
21[A]	12[A]	33[A]	21[H]	12[H]	33[H]	12[F]	33[F]	21[F]
31[A]	22[A]	13[A]	31[H]	22[H]	13[H]	22[F]	13[F]	31[F]
23[D]	11[D]	32[D]	32[B]	23[B]	11[B]	23[I]	11[I]	32[I]
33[D]	21[D]	12[D]	12[B]	33[B]	21[B]	33[I]	21[I]	12[I]
13[D]	31[D]	22[D]	22[B]	13[B]	31[B]	13[I]	31[I]	22[I]
32[G]	23[G]	11[G]	23[E]	11[E]	32[E]	11[C]	32[C]	23[C]
12[G]	33[G]	21[G]	33[E]	21[E]	12[E]	21[C]	12[C]	33[C]
22[G]	13[G]	31[G]	13[E]	31[E]	22[E]	31[C]	22[C]	13[C]

(b)

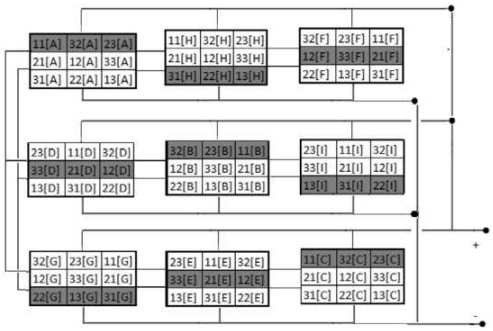

(c)

Figure 4.8: Short and Wide shading pattern: (a) S-M-TCT physical arrangement; (b) S-M-TCT electrical connection; (c) // S-M-TCT electrical connection.

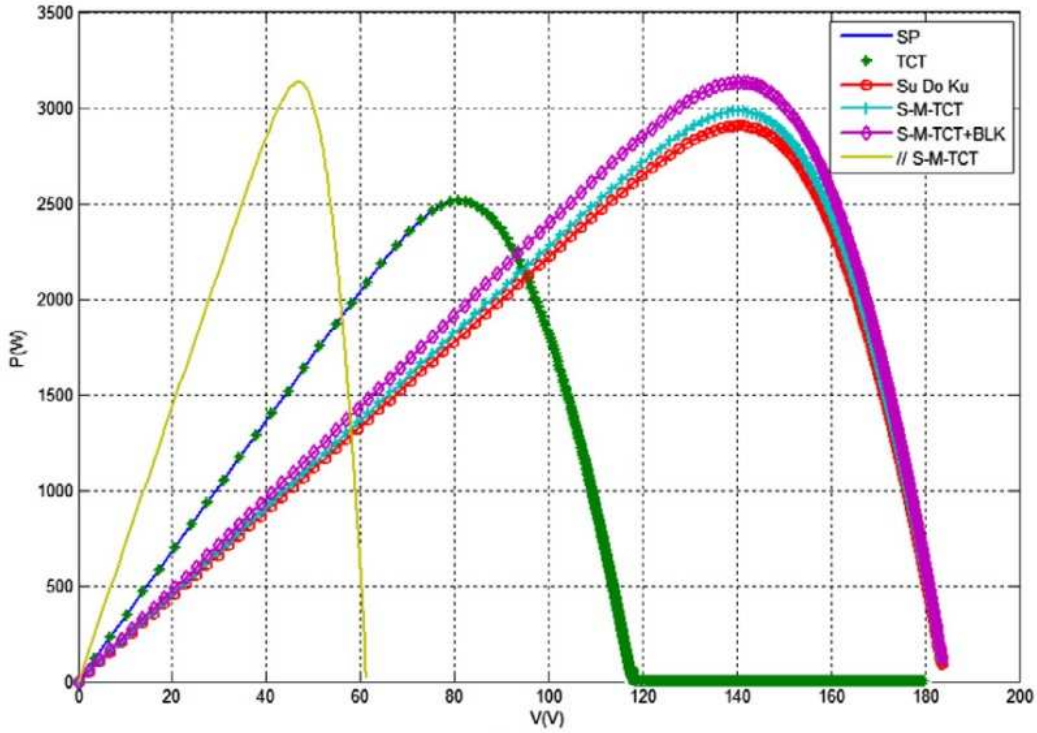

Figure 4.9: The P-V characteristics of different PV configuration of Short and Wide shading pattern.

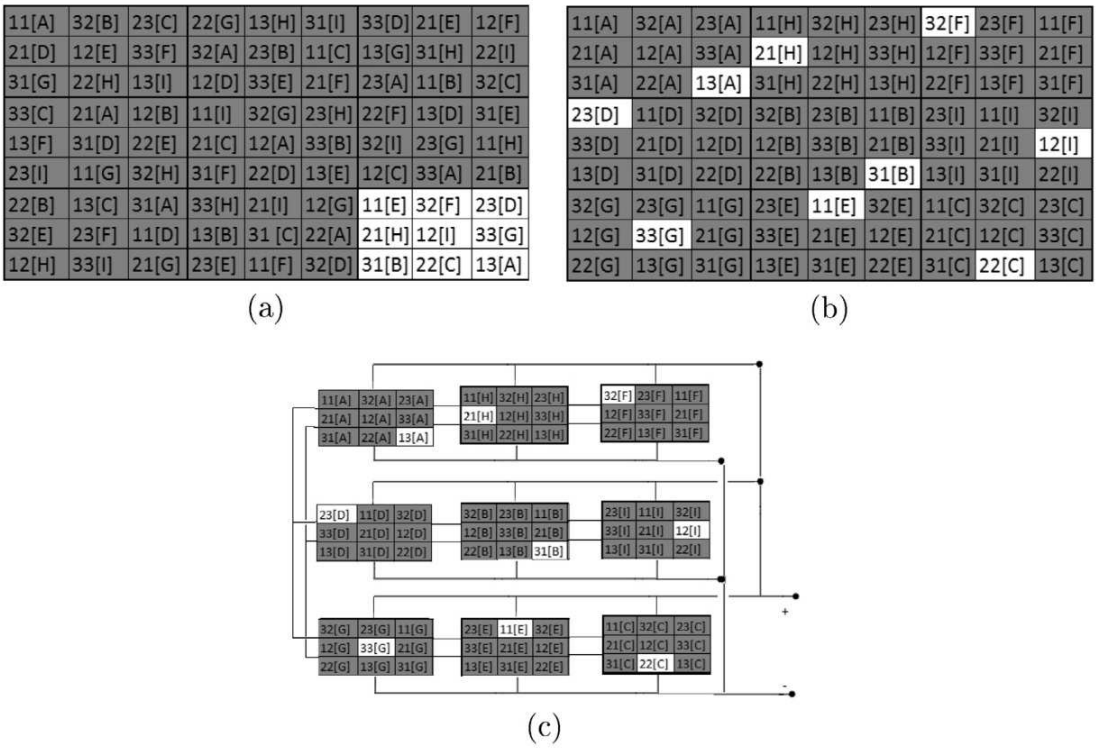

Figure 4.10: Wide and Long shading pattern: (a) S-M-TCT physical arrangement; (b) S-M-TCT electrical connection; (c) // S-M-TCT electrical connection.

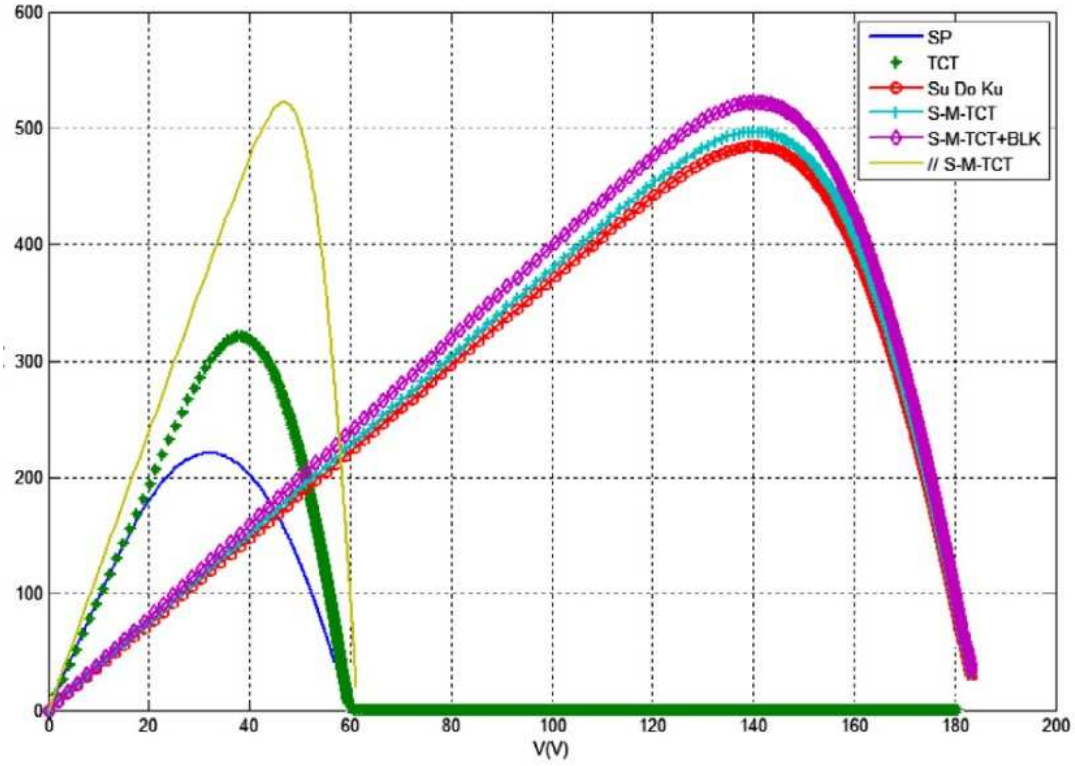

Figure 4.11: The P-V characteristics of different PV configuration of Wide and Long shading pattern.

4.3.5 Partial shading pattern scenarios with different irradiation levels

The shading pattern with different irradiance levels can not only reduce the PV array output but exhibit multi LMPPs on the P-V characteristic curve, which is its major impact. As a consequence of this issue the conventional MPPT controller will be trapped on one of these LMPP peaks. However, all proposed S-M-TCT arrangement can overcome this problem, under given scenarios as seen in Fig.4.12(a),(e),(i) and (m) giving just one MPP peak on the P-V curve as shown in Fig.4.12(d),(h),(l) and (p). This is due mainly to the uniform distribution of the shading pattern whereas in Su Do Ku, TCT and SP configurations it is not satisfied . The exact GMPPs values, for all presented PV array configurations, are given in the Table.4.2, which shows that S-M-TCT arrangement still has the highest power output.

4.3.6 Partial shading pattern scenarios among the PV Sub Arrays

The three chosen shading scenarios, seen in the Fig.4.13, help us to see the impact of the dynamic shading pattern effect minimization thru the three proposed PV array arrangements. The shading PV modules positions in the scenario 05 are all along the diagonal (Fig.4.13(a)) and across two sub arrays in the scenario 06 (Fig.4.13(e)). Whereas in scenario 07, the shading pattern at the center of PV array is across the three sub arrays (Fig.4.13(i)). The S-M-TCT arrangement distributes the Shading pattern equally in each row and column of the PV array for all these scenarios as shown in Fig.4.13(b),(f) and (j). Furthermore, Su Do Ku arrangements cannot achieve the same equal distribution of shading patterns as shown in the Fig.4.13(b),(f) and (j). In addition, the numbers of shaded PV modules for each row are not equal. Consequently, the LMPPs exhibition on the P-V characteristic curve with big GMPP decreases.

The proposed S-M-TCT arrangements get the highest GMPP compared to other PV

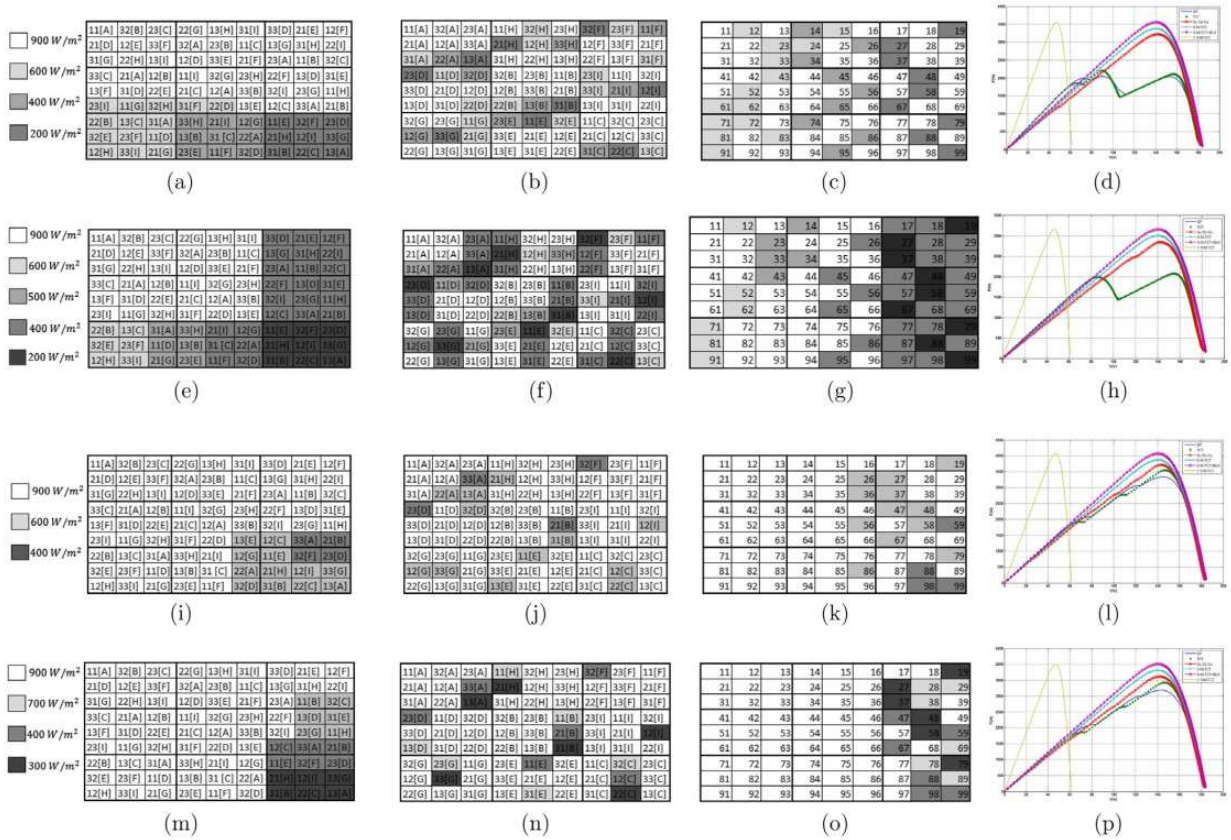

Figure 4.12: Shading pattern scenarios from 1 to 4 with different irradiation levels: S-M-TCT physical arrangement, shading dispersion using S-M-TCT arrangement, shading dispersion using Su Do Ku arrangement, P-V characteristics curves for SP, TCT, Su Do Ku, S-M-TCT, S-M-TCT+BLK, // S-M-TCT.

array configurations as shown in the Table.4.2. Furthermore, these arrangements eliminate the LMPPs compared to SP, TCT and Su Do Ku Fig.4.13(d),(h) and (l).

4.4 Proposed PV array arrangements: comparison and discussion

The GMPPs power outputs have been boosted for all the four-shadow types, under the given shadow pattern described in the previous sections by the proposed arrangements as shown in Fig. 4.14. The gains are higher compared to other configurations and

Shadow Types	MPP	SP	TCT	Sudoku	S-M-TCT	S-M-TCT+BLK	// S-M-TCT
Short & Narrow	(W)	2.9813e+03	3.3524e+03	3.9740e+03	3.9746e+03	4.0770e+03	4.0810e+03
	(%)	66.67 %	74.97 %	88.84 %	88.88 %	91.14 %	91.20 %
Narrow & Long	(W)	2.9813e+03	3.1498e+03	3.4409e+03	3.4780e+03	3.5487e+03	3.5519e+03
	(%)	66.67 %	70.44 %	76.51 %	77.77 %	79.35 %	79.40 %
Short & Wide	(W)	2.5138e+03	2.5138e+03	2.9755e+03	2.9996e+03	3.1315e+03	3.1319e+03
	(%)	56.20 %	56.20 %	66.54 %	67.08 %	70.00 %	70.01%
Wide & Long	(W)	220.9368	321.1002	471.8962	496.8783	538.3461	538.9947
	(%)	4.94 %	7.18 %	10.55 %	11.10 %	12.03 %	12.05%
Shading Scenario 01	(W)	2.0404e+03	2.2071e+03	3.2232e+03	3.3820e+03	3.5035e+03	3.5054e+03
	(%)	45.61 %	49.34 %	72.05%	75.61%	78.31 %	78.34 %
Shading Scenario 02	(W)	2.0626e+03	2.0754e+03	2.8428e+03	2.8739e+03	3.0528e+03	3.0532e+03
	(%)	46.11%	46.39%	63.55 %	64.25 %	68.25 %	68.27 %
Shading Scenario 03	(W)	3.3379e+03	3.5501e+03	3.8239e+03	3.8628e+03	4.0048e+03	4.0050e+03
	(%)	74.62 %	79.36 %	85.49 %	86.36 %	89.53%	89.54%
Shading Scenario 04	(W)	3.1905e+03	3.4237e+03	3.7148e+03	3.8136e+03	3.9481e+03	3.9489e+03
	(%)	71.32 %	76.54 %	83.05%	85.25%	88.26 %	88.28
Shading Scenario 05	(W)	3.8169e+03	3.9740e+03	3.7581e+03	3.9746e+03	4.0256e+03	4.0265e+03
	(%)	85.35 %	88.87 %	84.04 %	88.88 %	90.00 %	90.02 %
Shading Scenario 06	(W)	2.9813e+03	3.3524e+03	3.7581e+03	3.9746e+03	4.0761e+03	4.0772e+03
	(%)	66.67 %	74.97 %	83.97%	88.88 %	91.12 %	91.15 %
Shading Scenario 07	(W)	2.6246e+03	2.5842e+03	3.2756e+03	3.4780e+03	3.5487e+03	3.5490e+03
	(%)	58.69 %	57.79 %	73.25 %	77.77 %	79.35 %	79.36 %

Table 4.2: GMPP of different proposed configurations and arrangement under different shading pattern and scenarios .

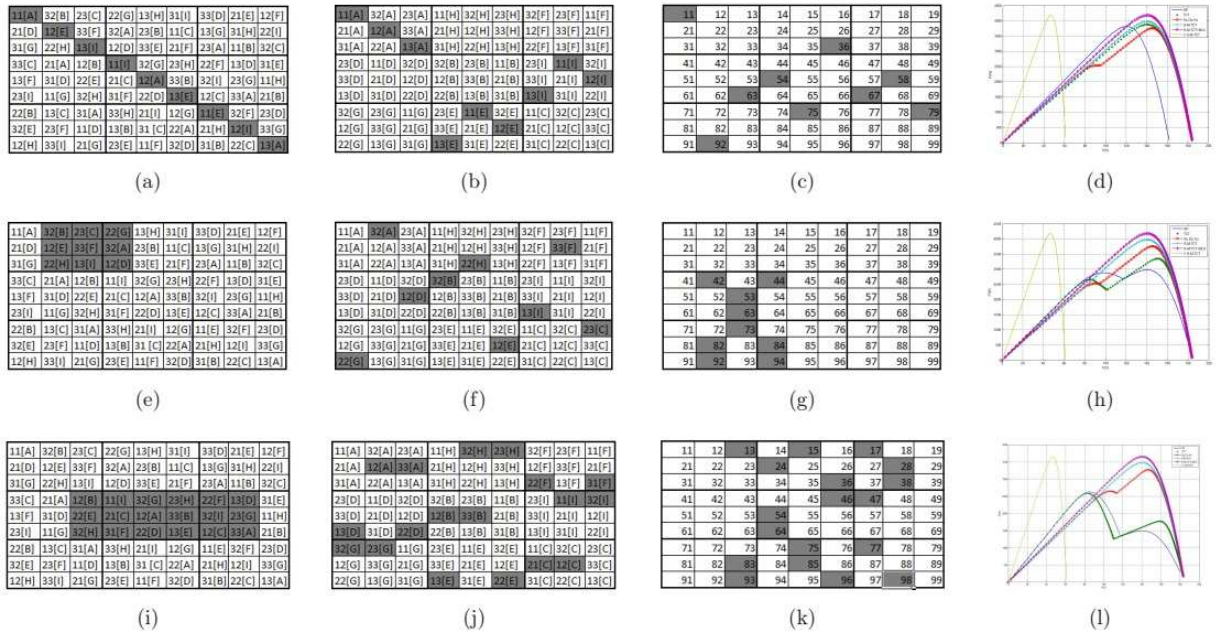

Figure 4.13: Shading pattern scenarios 5 to 7: S-M-TCT physical arrangement; shading dispersion using S-M-TCT arrangement; shading dispersion using Su do ku arrangement; P-V characteristics curves for SP, TCT, Su Do Ku, S-M-TCT, S-M-TCT+BLK, // S-M-TCT.

arrangements. In addition, the other shading scenarios GMPPs' are either summarized in the Fig. 4.14. These results prove that the proposed PV array arrangements still allow to get the highest power output whatever the shading pattern shape or the different irradiance levels.

Simulations show that the new PV array arrangements (S-M-TCT, //S-M-TCT and S-M-TCT+BLK) are effective in reducing the impact of the partial shading. A particularly significant result, obtained from the systematic assessment is that the proposed technique outperforms previous techniques under all scenarios since the multi-peaks problem is eliminated by the proposed PV array arrangements. So effectively, the tracking of the GMPP, with simple algorithms is possible with no need for complicated and costly MPPT controller based on complex algorithms.

Regarding PV array power output, we observe that // S-M-TCT and S-M-TCT+BLK have achieved almost the same GMPP (with a small difference of 1 %, due to the

blocking diodes power dissipation). Both techniques outperform S-M-TCT PV array arrangement in terms of power output.

The // S-M-TCT modifies the initial S-M-TCT PV array size, since all S-M-TCT sub arrays are connected in parallel. The new PV array column number increases and the number of rows decreases. This reduces the voltage and raises the current. Furthermore, if the PV system, with // S-M-TCT PV array arrangement, is required to feed a load, (e.g. battery or grid connected appliance) with specific value requirements for power, then voltage and current, should be matched to the load. The cost of the power converter to adapt the load to the PV array output should be taken in consideration. Such a power converter is not considered in either S-M-TCT or S-M-TCT+BLK PV array arrangements. The S-M-TCT+BLK PV array arrangement is based on the same S-M-TCT PV array arrangement; the only difference are the blocking diodes in the top of each PV module. The insertions of blocking diodes improve the S-M-TCT PV array energy yield and minimize the partial shading effect. The additional cost of blocking diodes is minimal since they are inexpensive. it is worth noting that all proposed PV array arrangements have generally the same interconnections and total wiring since they are all connected under a TCT configuration. They will therefore have the same total wire resistance.

4.5 Conclusion

This chapter proposes a new PV array physical arrangements in order to maximize the PV array power output and minimize the partial shading effect.

The proposed three arrangements (S-M-TCT, S-M-TCT+BLK and // S-M-TCT) show their efficiency compared to the existing PV configuration. In this approach, the physical arrangements of the PV modules within the PV array are in agreement with S-M-TCT, S-M-TCT+BLK and // S-M-TCT without altering the electrical connection. These arrangements distribute the partial shading pattern over the PV array to reduce the impact of shadow and increase the PV array output power. The performance of the

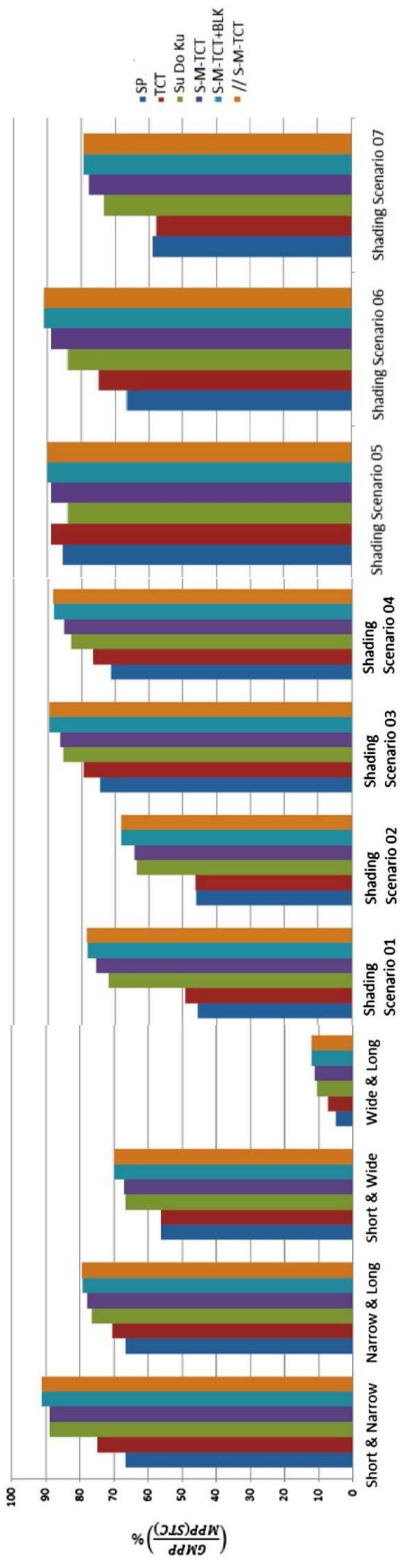

Figure 4.14: GMPP (%) for the various configurations and arrangements under different shadow types and shadow patterns scenarios.

proposed arrangements is studied and compared to different configurations for different shading patterns and scenarios.

The S-M-TCT PV array arrangements show better performance under partially shaded conditions compared to other PV configuration.

General conclusion and future works

The main aim of this thesis is to propose three new physical PV array arrangements (S-M-TCT, S-M-TCT+BLK and // S-M-TCT), without changing electrical connections. These arrangements can be applied to PV arrays of any size but, at this time, it has been tested on a 9x9 PV array. The proposed PV array arrangements were systematically analyzed under a range of shading scenarios and compared to several existing techniques/arrangements; they enhance the PV power output, minimize the protection diode power dissipation and eliminate the multiple peaks (LMPP) in the P-V characteristics curve under severe partial shading conditions. An alternative approach, to overcome the cost drawback of EAR and to achieve a balance between cost/complexity versus efficiency, is to use static reconfigurations. This approach consists of finding a PV module arrangement with a fixed predefined Total Cross Tied configuration. This predefined reconfiguration is designed such that the shading effect is minimized for a variety of shading patterns. Su DO Ku puzzle pattern is shown to effectively mitigate partial shading and maximize power PV generation. However, a Su Do Ku puzzle pattern is applicable only to 9x9 PV modules, and furthermore the impact of protection diodes, especially blocking diodes, needs to be taken into consideration. These techniques operate with an array of equal numbers of rows and columns, and are restricted to modifying the electrical connections of PV modules which are in the same physical PV array row. As a consequence, shading dispersion is limited and protection diodes power consumption is high.

The proposed arrangement distributes the shading pattern uniformly over the entire PV array so that the shaded PV module numbers are equal in rows and columns. As a

consequence, It generates a single MPP that corresponds to the GMPP, allowing the use of a simple MPPT controller that can track the MPP easily without the need for complex algorithms and costly hardware.

Overall, the different proposed S-M-TCT arrangements enhance GMPP for all presented shading pattern compared to other PV arrangements and configurations. More details for other configurations comparison under shading pattern and scenarios are given in the table.4.2. Though the analysis and performance was presented for up to 9x9 PV array sizes, the proposed arrangement is not limited to these arrays sizes. The generalization of the proposed arrangement to any arbitrary PV array size, by developing an algorithm, will be the focus of future works.

BIBLIOGRAPHY

[1] D. La Manna, V. L. Vigni, E. R. Sanseverino, V. Di Dio, and P. Romano, "Reconfigurable electrical interconnection strategies for photovoltaic arrays: A review," *Renewable and Sustainable Energy Reviews*, vol. 33, pp. 412–426, 2014.

[2] Y. Kuang, Y. Zhang, B. Zhou, C. Li, Y. Cao, L. Li, and L. Zeng, "A review of renewable energy utilization in islands," *Renewable and Sustainable Energy Reviews*, vol. 59, pp. 504–513, 2016.

[3] Y. Cancino-Solórzano, J. P. Paredes-Sánchez, A. J. Gutiérrez-Trashorras, and J. Xiberta-Bernat, "The development of renewable energy resources in the state of veracruz, mexico," *Utilities Policy*, vol. 39, pp. 1–4, 2016.

[4] S. K. Sahoo, "Renewable and sustainable energy reviews solar photovoltaic energy progress in india: A review," *Renewable and Sustainable Energy Reviews*, vol. 59, pp. 927–939, 2016.

[5] S. Pareek and R. Dahiya, "Enhanced power generation of partial shaded photovoltaic fields by forecasting the interconnection of modules," *Energy*, vol. 95, pp. 561–572, 2016.

[6] A. Murtaza, M. Chiaberge, F. Spertino, D. Boero, and M. De Giuseppe, "A maximum power point tracking technique based on bypass diode mechanism for pv arrays under partial shading," *Energy and Buildings*, vol. 73, pp. 13–25, 2014.

[7] S. A. Rizzo and G. Scelba, "Ann based mppt method for rapidly variable shading conditions," *Applied Energy*, vol. 145, pp. 124–132, 2015.

[8] B. N. Alajmi, K. H. Ahmed, S. J. Finney, and B. W. Williams, "A maximum power point tracking technique for partially shaded photovoltaic systems in microgrids," *IEEE Transactions on Industrial Electronics*, vol. 60, no. 4, pp. 1596–1606, 2013.

[9] K. Ishaque and Z. Salam, "A review of maximum power point tracking techniques of pv system for uniform insolation and partial shading condition," *Renewable and Sustainable Energy Reviews*, vol. 19, pp. 475–488, 2013.

[10] Y.-H. Liu, C.-L. Liu, J.-W. Huang, and J.-H. Chen, "Neural-network-based maximum power point tracking methods for photovoltaic systems operating under fast changing environments," *Solar Energy*, vol. 89, pp. 42–53, 2013.

[11] S. Daraban, D. Petreus, and C. Morel, "A novel mppt (maximum power point tracking) algorithm based on a modified genetic algorithm specialized on tracking the global maximum power point in photovoltaic systems affected by partial shading," *Energy*, vol. 74, pp. 374–388, 2014.

[12] S. N. Deshkar, S. B. Dhale, J. S. Mukherjee, T. S. Babu, and N. Rajasekar, "Solar pv array reconfiguration under partial shading conditions for maximum power extraction using genetic algorithm," *Renewable and Sustainable Energy Reviews*, vol. 43, pp. 102–110, 2015.

[13] L. F. L. Villa, D. Picault, B. Raison, S. Bacha, and A. Labonne, "Maximizing the power output of partially shaded photovoltaic plants through optimization of the interconnections among its modules," *Photovoltaics, IEEE Journal of*, vol. 2, no. 2, pp. 154–163, 2012.

[14] S. Malathy and R. Ramaprabha, "Comprehensive analysis on the role of array size and configuration on energy yield of photovoltaic systems under shaded conditions," *Renewable and Sustainable Energy Reviews*, vol. 49, pp. 672–679, 2015.

[15] G. Velasco-Quesada, F. Guinjoan-Gispert, R. Pique-Lopez, M. Roman-Lumbreras, and A. Conesa-Roca, "Electrical pv array reconfiguration strategy for energy extraction improvement in grid-connected pv systems," *IEEE Transactions on Industrial Electronics*, vol. 56, no. 11, pp. 4319–4331, 2009.

[16] S. R. Potnuru, D. Pattabiraman, S. I. Ganesan, and N. Chilakapati, "Positioning of pv panels for reduction in line losses and mismatch losses in pv array," *Renewable Energy*, vol. 78, pp. 264–275, 2015.

[17] H. S. Sahu and S. K. Nayak, "Power enhancement of partially shaded pv array by using a novel approach for shade dispersion," in *Innovative Smart Grid Technologies-Asia (ISGT Asia), 2014 IEEE*, pp. 498–503, IEEE, 2014.

[18] K. Ishaque, Z. Salam, and H. Taheri, "Simple, fast and accurate two-diode model for photovoltaic modules," *Solar Energy Materials and Solar Cells*, vol. 95, no. 2, pp. 586–594, 2011.

[19] K. Ishaque, Z. Salam, H. Taheri, *et al.*, "Modeling and simulation of photovoltaic (pv) system during partial shading based on a two-diode model," *Simulation Modelling Practice and Theory*, vol. 19, no. 7, pp. 1613–1626, 2011.

[20] K. Ishaque, Z. Salam, *et al.*, "A comprehensive matlab simulink pv system simulator with partial shading capability based on two-diode model," *Solar Energy*, vol. 85, no. 9, pp. 2217–2227, 2011.

[21] N. Belhaouas, M.-S. Ait Cheikh, and C. Larbes, "Suitable matlab-simulink simulator for pv system based on a two-diode model under shading conditions," in *Systems and Control (ICSC), 2013 3rd International Conference on*, pp. 72–76, IEEE, 2013.

[22] D. S. Chan and J. C. Phang, "Analytical methods for the extraction of solar-cell single-and double-diode model parameters from iv characteristics," *Electron Devices, IEEE Transactions on*, vol. 34, no. 2, pp. 286–293, 1987.

[23] D. H. Muhsen, A. B. Ghazali, T. Khatib, and I. A. Abed, "Parameters extraction of double diode photovoltaic moduleís model based on hybrid evolutionary algorithm," *Energy Conversion and Management*, vol. 105, pp. 552–561, 2015.

[24] M. Hejri, H. Mokhtari, M. Azizian, M. Ghandhari, and L. Soder, "On the parameter extraction of a five-parameter double-diode model of photovoltaic cells and modules," *Photovoltaics, IEEE Journal of*, vol. 4, pp. 915–923, May 2014.

[25] V. L. Brano and G. Ciulla, "An efficient analytical approach for obtaining a five parameters model of photovoltaic modules using only reference data," *Applied Energy*, vol. 111, pp. 894–903, 2013.

[26] E. Karatepe, M. Boztepe, and M. Colak, "Development of a suitable model for characterizing photovoltaic arrays with shaded solar cells," *Solar Energy*, vol. 81, no. 8, pp. 977–992, 2007.

[27] S. Said, A. Massoud, M. Benammar, and S. Ahmed, "A matlab/simulink based photovoltaic array model. employing simpowersystems toolbox," *Journal of Energy and Power Engineering*, vol. 6, no. 12, pp. 1965–1975, 2012.

[28] E. Q. B. Macabebe, C. J. Sheppard, and E. E. van Dyk, "Parameter extraction from i–v characteristics of pv devices," *Solar Energy*, vol. 85, no. 1, pp. 12–18, 2011.

[29] V. Quaschning and R. Hanitsch, "Numerical simulation of current-voltage characteristics of photovoltaic systems with shaded solar cells," *Solar Energy*, vol. 56, no. 6, pp. 513–520, 1996.

[30] M. A. Eltawil and Z. Zhao, "Mppt techniques for photovoltaic applications," *Renewable and Sustainable Energy Reviews*, vol. 25, pp. 793–813, 2013.

[31] Y.-H. Liu, J.-H. Chen, and J.-W. Huang, "A review of maximum power point tracking techniques for use in partially shaded conditions," *Renewable and Sustainable Energy Reviews*, vol. 41, pp. 436–453, 2015.

[32] F. Chekired, A. Mellit, S. Kalogirou, and C. Larbes, "Intelligent maximum power point trackers for photovoltaic applications using fpga chip: A comparative study," *Solar Energy*, vol. 101, pp. 83–99, 2014.

[33] J. Ahmed and Z. Salam, "A critical evaluation on maximum power point tracking methods for partial shading in pv systems," *Renewable and Sustainable Energy Reviews*, vol. 47, pp. 933–953, 2015.

[34] S. Titri, C. Larbes, K. Y. Toumi, and K. Benatchba, "A new mppt controller based on the ant colony optimization algorithm for photovoltaic systems under partial shading conditions," *Applied Soft Computing*, vol. 58, pp. 465–479, 2017.

[35] F. Belhachat and C. Larbes, "Global maximum power point tracking based on anfis approach for pv array configurations under partial shading conditions," *Renewable and Sustainable Energy Reviews*, vol. 77, pp. 875–889, 2017.

[36] D. Sera, L. Mathe, T. Kerekes, S. V. Spataru, and R. Teodorescu, "On the perturb-and-observe and incremental conductance mppt methods for pv systems," *IEEE journal of photovoltaics*, vol. 3, no. 3, pp. 1070–1078, 2013.

[37] J. Ahmed and Z. Salam, "An improved perturb and observe (p&o) maximum power point tracking (mppt) algorithm for higher efficiency," *Applied Energy*, vol. 150, pp. 97–108, 2015.

[38] A. Safari and S. Mekhilef, "Simulation and hardware implementation of incremental conductance mppt with direct control method using cuk converter," *IEEE transactions on industrial electronics*, vol. 58, no. 4, pp. 1154–1161, 2011.

[39] B. Liu, S. Duan, F. Liu, and P. Xu, "Analysis and improvement of maximum power point tracking algorithm based on incremental conductance method for photovoltaic array," in *Power Electronics and Drive Systems, 2007. PEDS'07. 7th International Conference on*, pp. 637–641, IEEE, 2007.

[40] M. Birane, C. Larbes, and A. Cheknane, "Comparative study and performance evaluation of central and distributed topologies of photovoltaic system," *International Journal of Hydrogen Energy*, vol. 42, no. 13, pp. 8703–8711, 2017.

[41] H. Patel and V. Agarwal, "Matlab-based modeling to study the effects of partial shading on pv array characteristics," *IEEE Transactions on Energy Conversion*, vol. 23, no. 1, pp. 302–310, 2008.

[42] J. Bai, Y. Cao, Y. Hao, Z. Zhang, S. Liu, and F. Cao, "Characteristic output of pv systems under partial shading or mismatch conditions," *Solar Energy*, vol. 112, pp. 41–54, 2015.

[43] D. Rossi, M. Omana, D. Giaffreda, and C. Metra, "Modeling and detection of hotspot in shaded photovoltaic cells," *Very Large Scale Integration (VLSI) Systems, IEEE Transactions on*, vol. 23, pp. 1031–1039, June 2015.

[44] S. Spanoche, J. Stewart, S. Hawley, and I. Opris, "Model-based method for partially shaded pv module hot-spot suppression," *Photovoltaics, IEEE Journal of*, vol. 3, pp. 785–790, April 2013.

[45] V. d'Alessandro, P. Guerriero, and S. Daliento, "A simple bipolar transistor-based bypass approach for photovoltaic modules," *Photovoltaics, IEEE Journal of*, vol. 4, pp. 405–413, Jan 2014.

[46] S. Silvestre, A. Boronat, and A. Chouder, "Study of bypass diodes configuration on pv modules," *Applied Energy*, vol. 86, no. 9, pp. 1632–1640, 2009.

[47] K. Kim and P. Krein, "Reexamination of photovoltaic hot spotting to show inadequacy of the bypass diode," *Photovoltaics, IEEE Journal of*, vol. 5, pp. 1435–1441, Sept 2015.

[48] H. Zheng, S. Li, R. Challoo, and J. Proano, "Shading and bypass diode impacts to energy extraction of pv arrays under different converter configurations," *Renewable Energy*, vol. 68, pp. 58–66, 2014.

[49] L. Gao, R. A. Dougal, S. Liu, and A. P. Iotova, "Parallel-connected solar pv system to address partial and rapidly fluctuating shadow conditions," *IEEE Transactions on Industrial Electronics*, vol. 56, pp. 1548–1556, May 2009.

[50] M. S. El-Dein, M. Kazerani, and M. Salama, "Optimal photovoltaic array reconfiguration to reduce partial shading losses," *Sustainable Energy, IEEE Transactions on*, vol. 4, no. 1, pp. 145–153, 2013.

[51] A. Woyte, J. Nijs, and R. Belmans, "Partial shadowing of photovoltaic arrays with different system configurations: literature review and field test results," *Solar Energy*, vol. 74, no. 3, pp. 217–233, 2003.

[52] A. J. Hanson, C. Deline, S. M. MacAlpine, J. T. Stauth, C. R. Sullivan, *et al.*, "Partial-shading assessment of photovoltaic installations via module-level monitoring," *Photovoltaics, IEEE Journal of*, vol. 4, no. 6, pp. 1618–1624, 2014.

[53] Y.-J. Wang and S.-S. Lin, "Analysis of a partially shaded pv array considering different module connection schemes and effects of bypass diodes," in *Utility Exhibition on Power and Energy Systems: Issues & Prospects for Asia (ICUE), 2011 International Conference and*, pp. 1–7, IEEE, 2011.

[54] F. Belhachat and C. Larbes, "Modeling, analysis and comparison of solar photovoltaic array configurations under partial shading conditions," *Solar Energy*, vol. 120, pp. 399–418, 2015.

[55] R. Kadri, H. Andrei, J.-P. Gaubert, T. Ivanovici, G. Champenois, and P. Andrei, "Modeling of the photovoltaic cell circuit parameters for optimum connection model and real-time emulator with partial shadow conditions," *Energy*, vol. 42, no. 1, pp. 57–67, 2012.

[56] L. F. L. Villa, T.-P. Ho, J.-C. Crebier, and B. Raison, "A power electronics equalizer application for partially shaded photovoltaic modules," *Industrial Electronics, IEEE Transactions on*, vol. 60, no. 3, pp. 1179–1190, 2013.

[57] K. Ş. Parlak, "Pv array reconfiguration method under partial shading conditions," *International Journal of Electrical Power & Energy Systems*, vol. 63, pp. 713–721, 2014.

[58] P. Srinivasa Rao, G. Saravana Ilango, and C. Nagamani, "Maximum power from pv arrays using a fixed configuration under different shading conditions," *Photovoltaics, IEEE Journal of*, vol. 4, pp. 679–686, March 2014.

[59] B. I. Rani, G. S. Ilango, and C. Nagamani, "Enhanced power generation from pv array under partial shading conditions by shade dispersion using su do ku configuration," *IEEE Transactions on Sustainable Energy*, vol. 4, no. 3, pp. 594 – 601, 2013.

[60] B. Celik, E. Karatepe, S. Silvestre, N. Gokmen, and A. Chouder, "Analysis of spatial fixed pv arrays configurations to maximize energy harvesting in bipv applications," *Renewable Energy*, vol. 75, pp. 534–540, 2015.

[61] H. Tian, F. Mancilla-David, K. Ellis, E. Muljadi, and P. Jenkins, "Determination of the optimal configuration for a photovoltaic array depending on the shading condition," *Solar Energy*, vol. 95, pp. 1–12, 2013.